NASA CONTRACTOR REPORT

CR-61129

CR-61129

INTERPLANETARY NAVIGATION AND GUIDANCE STUDY VOLUME I: SUMMARY

Prepared under Contract No. NAS 8-11198 by

PHILCO CORPORATION

For

NASA-GEORGE C. MARSHALL SPACE FLIGHT CENTER
Huntsville, Alabama

March 28, 1966

CR-61129

INTERPLANETARY NAVIGATION AND GUIDANCE STUDY

VOLUME I: SUMMARY

(Report Dated October 30, 1965)

Prepared under Contract No. NAS 8-11198 by

PHILCO CORPORATION

For

Astrionics Laboratory

NASA-GEORGE C. MARSHALL SPACE FLIGHT CENTER

ABSTRACT

This report is a summary of WDL-TR2629 Volumes II and III which contain the results of a study performed under Contract NAS8-11198. The primary purpose of the study is to establish the navigation and guidance system requirements for an Earth-Mars round-trip mission. A secondary purpose is to develop general analysis techniques that could be used to establish those requirements for any interplanetary mission.

The scope of the study includes a statistical error analysis of the navigation and guidance systems for the midcourse and orbital phases of the Earth-Mars mission. A 532 day round-trip trajectory is used which is based on a 1975 launch opportunity and has high energies for both the outbound and return phases. In general, only random errors resulting from the navigation instruments and the guidance maneuvers are considered. Four navigation system configurations are evaluated under the assumption that observation data are processed with a minimum variance Kalman filter to estimate the vehicle state.

Sections 2, 3, and 4 of this report summarize the navigation and guidance theory, the computer simulation, and the onboard measurement techniques that have been used in the study. The principal results are discussed in Sections 5, 6 and 7 for the outbound midcourse, the return midcourse phase, and the Mars orbital phase, respectively.

FOREWORD

This volume contains a summary of the navigation and guidance analysis performed under contracts NAS 8 11198 for Marshall Space Flight Center. The detailed analysis are presented in Volumes II and III.

TABLE OF CONTENTS

SECTION 1

INTRODUCTION

1.1 GENERAL OBJECTIVES AND SCOPE

The primary objective of contract NAS8-11198 is to establish the basic requirements for an Advanced Spaceborne Detection, Tracking and Navigation System capable of performing future interplanetary missions. To achieve this objective, the following tasks had to be completed:

a. Organize the study such that information is obtained which shows tradeoff between performance and system complexity, and can be used to select a system for a given mission.

b. Derive suitable mathematical techniques for calculating the guidance and navigation systems performance.

c. Develop methods for data presentation which indicate accuracy tradeoffs between various subsystems and components within a particular system.

d. Determine the areas and components which require future research.

The scope of the study includes an evaluation of systems which utilize Earth-based and onboard navigation, and combinations of the two systems. The results obtained can be used to establish the capabilities of these systems to perform various missions. In order to make the problem amenable to study, however, certain restrictions on the scope of the study had to be made. The following restrictions were either suggested by or approved by MSFC personnel:

a. Primary emphasis and calculations are for the 1975 opportunity for a round-trip to Mars (Figure 1-1). The trajectory includes a stay time of about 40 days in orbit about Mars at an altitude higher than the sensible Martian atmosphere (500 Km). The outbound flight time is 235 days, and the return flight time is 297 days. This restriction was made at the start of the study because obtaining data for all possible missions would not be feasible.

Some data are also generated for the round-trip trajectory shown in Figure 1-2. This is a 180-day low energy outbound trajectory with a 360-day return trajectory. The return trajectory includes a Venus swingby.

b. The covariance matrix of injection errors at the Earth is not studied as a parameter. This matrix, which is a function of the time in park orbit at the Earth, is intended to be representative of the capabilities of future launch vehicle guidance systems. The primary influence of this matrix is on the magnitude of the midcourse velocity requirements at the first guidance correction.

c. The study emphasized the following phases of the mission:
   1. Midcourse from Earth to Mars
   2. Orbital navigation at Mars
   3. Midcourse from Mars to Earth.

These phases are probably the most demanding on the sensor requirements if one neglects the inertial components required during the accelerating (or decelerating) positions of the total mission.

1.2 STUDY FORMAT

The requirements of the navigation and guidance systems may vary considerably depending on the mission itself. This study is designed to obtain data that shows the tradeoff between onboard system complexity and the guidance and navigation system performance that can be achieved. Four navigation system configurations are considered; they vary in complexity from one that depends entirely on Earth-based tracking and computations to one that has a total onboard navigation capability. These four systems could be used for missions that vary from a simple planetary flyby mission to a round-trip manned mission.

The four navigation and guidance systems whose performance are analyzed in this study are:

a. <u>System I</u>

1. Onboard Equipment
    (a) An attitude control system with a reference alignment procedure
    (b) Rocket motor for thrusting
    (c) Command system for receipt of command signals for midcourse maneuvers.
2. Earth-Based Equipment
    (a) DSIF Tracking Network
    (b) Computation facilities
3. Typical Mission
    (a) Planetary flyby
    (b) Planetary orbiter

b. <u>System II</u>

1. Onboard Equipment
    (a) Same as System I
    (b) Sextant or theodolite - Measurements restricted near maneuver times to permit Earth-based computation
2. Earth-Based Equipment
    (a) Same as System I
3. Typical Missions
    (a) Close Approach Flyby
    (b) Planetary Orbiter

c. <u>System III</u>

1. Onboard Equipment
    (a) Same as System II

(b) Onboard radar

(c) Digital computer which will be used during the terminal part of the outbound midcourse phase, orbital navigation phase, and the initial part of the midcourse return phase. This sytem would allow rapid onboard calculations when they are required during the rapidly changing portions of the flight which occur at great distances (and consequently cause command time delays) from the Earth.

2. Earth-Based Equipment

(a) Same as System II

3. Typical Mission

(a) Manned round-trip to Mars

(b) Planetary orbiter

(c) Lander

d. <u>System IV</u>

1. Onboard Equipment

(a) Same as System III with the exception of the command system; System IV places no reliance on Earth-based facilities.

2. Earth-Based Equipment

(a) None; complete onboard system for all phases of the mission

3. Typical Mission

(a) Manned round-trip to Mars

1.3 STUDY ASSUMPTIONS

The results of this study have been obtained with the following assumptions:

1) Linear theory applies in the neighborhood of the nominal trajectory. This allows the ensemble statistical data to be calculated efficiently for quantities such as RMS deviation from the nominal, RMS miss at the target, RMS midcourse velocity requirements, etc.

2) Navigation measurements are processed with Kalman Minimum Variance filter (weighted least squares or Maximum Likelihood are equally applicable).

3) Maneuvers may be represented by step changes in velocity. This permits the error sources to be represented by a simple but realistic mathematical model and simplifies the calculation of ensemble statistical data for the guidance system analysis.

4) Mathematical models of the error sources are constrained to those which the current simulation program can handle. The primary emphasis is on random error sources. The Earth-based tracker station location errors were treated as bias error sources but equation-of-motion uncertainties and measurement biases were neglected.

5) The error sources that are considered in the study are the following:

   (a) Onboard Control System (Random Errors)

      (1) Shut-off Error - proportional to and in the direction of velocity correction.

      (2) Resolution Error - independent of magnitude but in the direction of velocity correction.

      (3) Pointing Error - proportional to the magnitude and normal to direction of the velocity correction.

   (b) Earth-Based Tracking (Random Errors)

      (1) Range-rate

      (2) Azimuth

      (3) Elevation

   (c) Onboard Angular Measurements (Random Error - magnitude depends on planet subtended angle).

      (1) Right ascension, declination (theodolite).

      (2) Planet-star angle (sextant).

      (3) Subtended angle (range measurements).

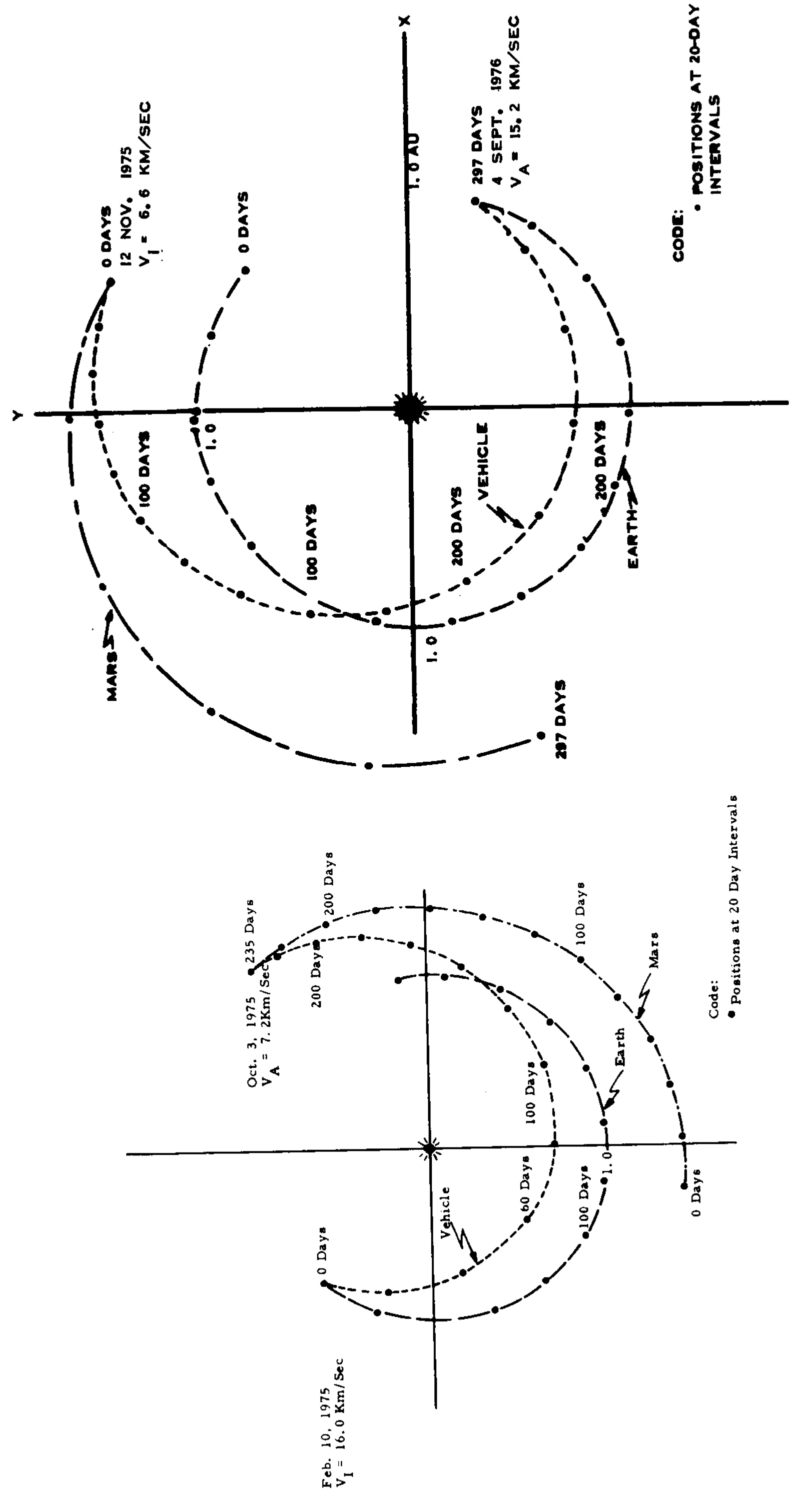

Figure 1-1 High-Energy Round-Trip Mars Trajectory

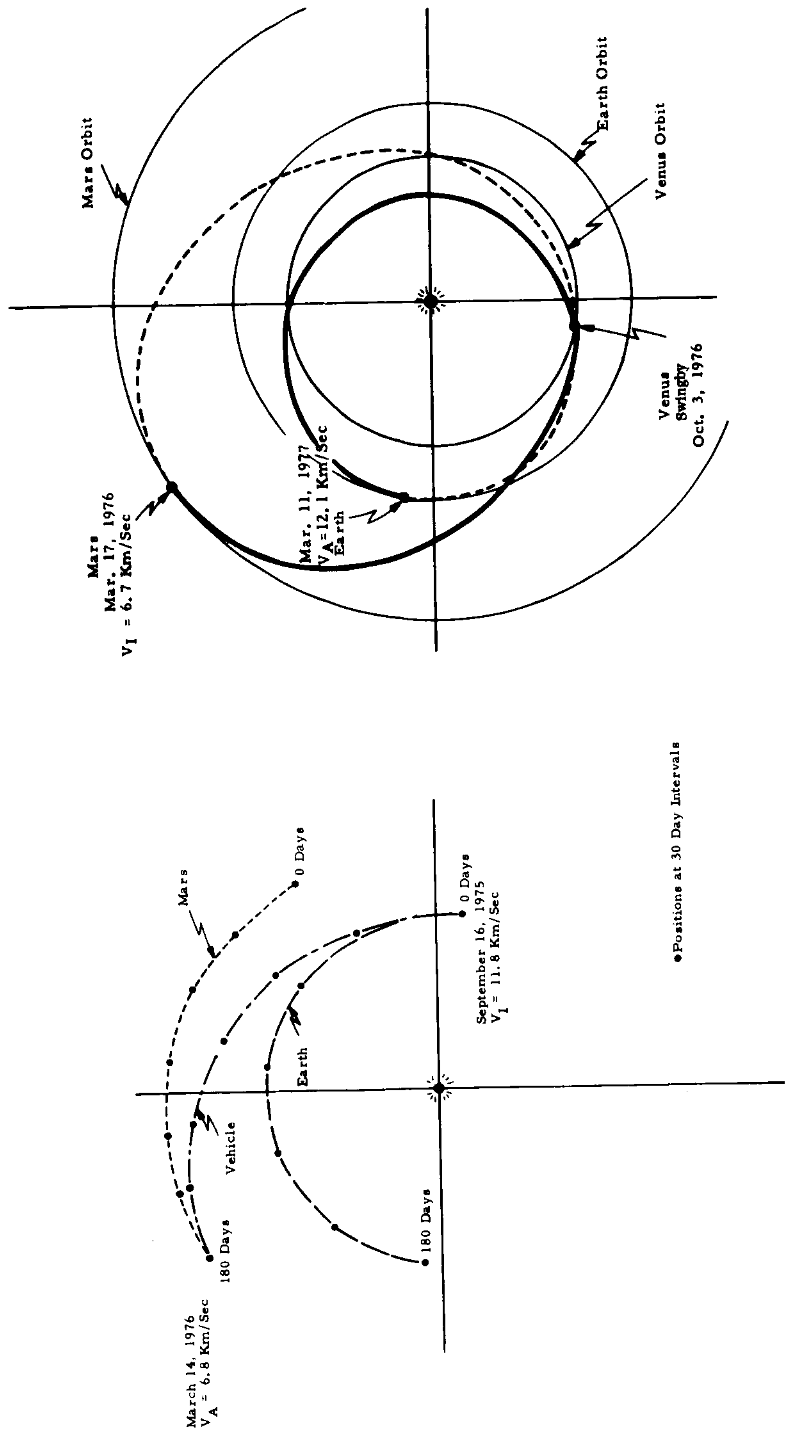

Figure 1-2 Low Energy Round-Trip Mars Trajectory

SECTION 2

THEORETICAL ANALYSIS OF THE NAVIGATION AND GUIDANCE SYSTEMS

This section presents a summary of the theoretical analysis* which is used to evaluate the navigation and guidance system capabilities in this study. Linear perturbation theory about a nominal trajectory is used to perform statistical analyses of the deviation state, x, (Figure 2-1). An estimate of the state, $\hat{x}$, is obtained by the navigation system as the result of taking observations and smoothing the data with a Kalman filter. The errors in estimates of the state $\tilde{x}$ indicate the performance of the navigation system. The estimate of the state $\hat{x}$ is used in computing guidance corrections. The ensemble statistical behavior of these deviation quantities can be determined in a linear system by analysis of their covariance matrices (Figure 2-2).

2.1 NAVIGATION SYSTEM

The equations below show the change in the deviation state estimate and covariance matrix of the error in estimate when a Kalman filter is used to include an observation in the estimate.

$$\hat{x}_n = \hat{x} + PH^T(HPH^T + Q)^{-1} (y-\hat{y}) \tag{2-1}$$

$$P_n = P - PH^T(HPH^T + Q)^{-1} HP \tag{2-2}$$

where

$\hat{x}_n$ = estimate of deviation state after an observation

$\hat{x}$ = old estimate of deviation state

P = covariance matrix of error in estimate of the state

* Derivations of equations are presented in Section 2.0 of Reference 1.

H = gradient of measurement with respect to the state (row vector)

Q = variance of measurement noise

y = measurement value

$\hat{y}$ = estimate of measurement value

P_n = covariance matrix of error in estimate of states after the observation.

The equations for the propagation of the deviation state estimate and covariance matrix of the error in estimate along the nominal trajectory (Figure 2-2) are the following:

$$\hat{x}(t_2) = \Phi(t_2;t_1)\ \hat{x}(t_1) \tag{2-3}$$

$$P(t_2) = \Phi(t_2;t_1)\ P(t_1)\ \Phi^T(t_2;t_1) \tag{2-4}$$

where $\Phi(t_2;t_1)$ is the transition matrix from time t_1 to time t_2.

The estimate of the terminal constraint deviation and covariance matrix of the error in estimate of deviations are obtained by using (2-3) and (2-4) with the transition matrix to the terminal time T and a point transformation between the terminal deviation state and the constraint deviation as follows:

$$\begin{bmatrix} \hat{\delta}\ \vec{B}\cdot\hat{T} \\ \hat{\delta}\ \vec{B}\cdot\hat{R} \\ \hat{\delta}\ V_{inf} \end{bmatrix} = C(T)\ \Phi(T;t)\ \hat{x}(t) = D(T,t)\ \hat{x}(t) \tag{2-5}$$

$$EST = C(T)\Phi(T;t)P(t)\Phi^T(T;t)C^T(T) \tag{2-6}$$

where

$C(T)$ = point transformation from state deviations to constraint deviations

EST = covariance matrix of error in estimate of end constraints.

2.2 GUIDANCE SYSTEM

The linear analysis of the guidance system is summarized by the following equations:

$$\hat{\dot{\underline{x}}}_g(t) = -D_2^{-1}C(T)\hat{x}(T) \tag{2-7}$$

$$E(\hat{\dot{\underline{x}}}_g\hat{\dot{\underline{x}}}_g^T) = -D_2^{-1}C(T)\left\{PAR(T) - P(T)\right\}C^T(T)\left[D_2^{-1}\right]^T \tag{2-8}$$

where

$\hat{\dot{\underline{x}}}_g(t)$ = the estimated velocity correction required

D_2 = matrix of sensitivities relating constraint changes at time T to velocity changes at time t.

$E(\hat{\dot{\underline{x}}}_g\hat{\dot{\underline{x}}}_g^T)$ = covariance matrix of the estimated velocity correction.

The selection of the terminal constraints which are to be controlled establish the guidance law. The three guidance laws considered in this study are shown pictorially in Figure 2-3.

The P and PAR covariance matrices following a guidance correction are as follows (Figure 2-2B):

$$PAR_A = P_B + \begin{bmatrix} 0 & 0 \\ 0 & E(\epsilon\epsilon^T) \end{bmatrix} \tag{2-9}$$

$$P_A = P_B + \alpha \begin{bmatrix} 0 & 0 \\ 0 & E(\epsilon\epsilon^T) \end{bmatrix} \tag{2-10}$$

where the subscripts A and B refer to after the correction and before the correction respectively, and $E(\epsilon\epsilon^T)$ is the covariance matrix of the execution errors (proportional,resolution,and pointing).

The state deviations described by (2-9) are with respect to the new nominal trajectory defined at the time of the correction based on the estimate of the state at that time. The quantity α in (2-10) is a constant that may assume values from 0 to 1. It is the result of monitoring the guidance correction with an onboard device.

2.3 END CONSTRAINTS

The results of this study are presented in terms of the end constraints which have been used. The end position state used with the Fixed Time of Arrival (FTA) guidance law was expressed in altitude, down range, and cross range coordinates of periapsis (Figure 2-4A).

The $\vec{B}$ vector[2] was used to control the target passage distance with the Variable Time of Arrival guidance law (Figure 2-4B). The $\hat{T}$ and $\hat{R}$ vectors are selected (Figure 2-4B) so deviations in $\vec{B}\cdot\hat{T}$ are deviations in the magnitude of the $\vec{B}$ vector and deviations in $\vec{B}\cdot\hat{R}$ are deviations in the inclination of the approach trajectory plane. The deviations in $\vec{B}\cdot\hat{T}$ for this case can be expressed as deviations in radius of closest approach or periapsis altitude deviations. The relationship is shown below[3]:

$$|\vec{B}| = r_A \sqrt{1 + \frac{2\mu}{r_A v_\infty^2}} \tag{2-11}$$

$$\frac{\partial |\vec{B}|}{\partial r_A} = \left[\frac{|\vec{B}|}{r_A} - \frac{\mu}{|\vec{B}| v_\infty^2}\right] = \frac{\partial\, \vec{B}\cdot\hat{T}}{\partial r_A} \tag{2-12}$$

where

r_A = radius of closest approach

μ = gravitation constant

v_∞ = velocity at infinite distance

For the nominal trajectories that have been used for the outbound and return phases, the closest approach deviations are approximately .95 of the $\vec{B}\cdot\hat{T}$ deviations.

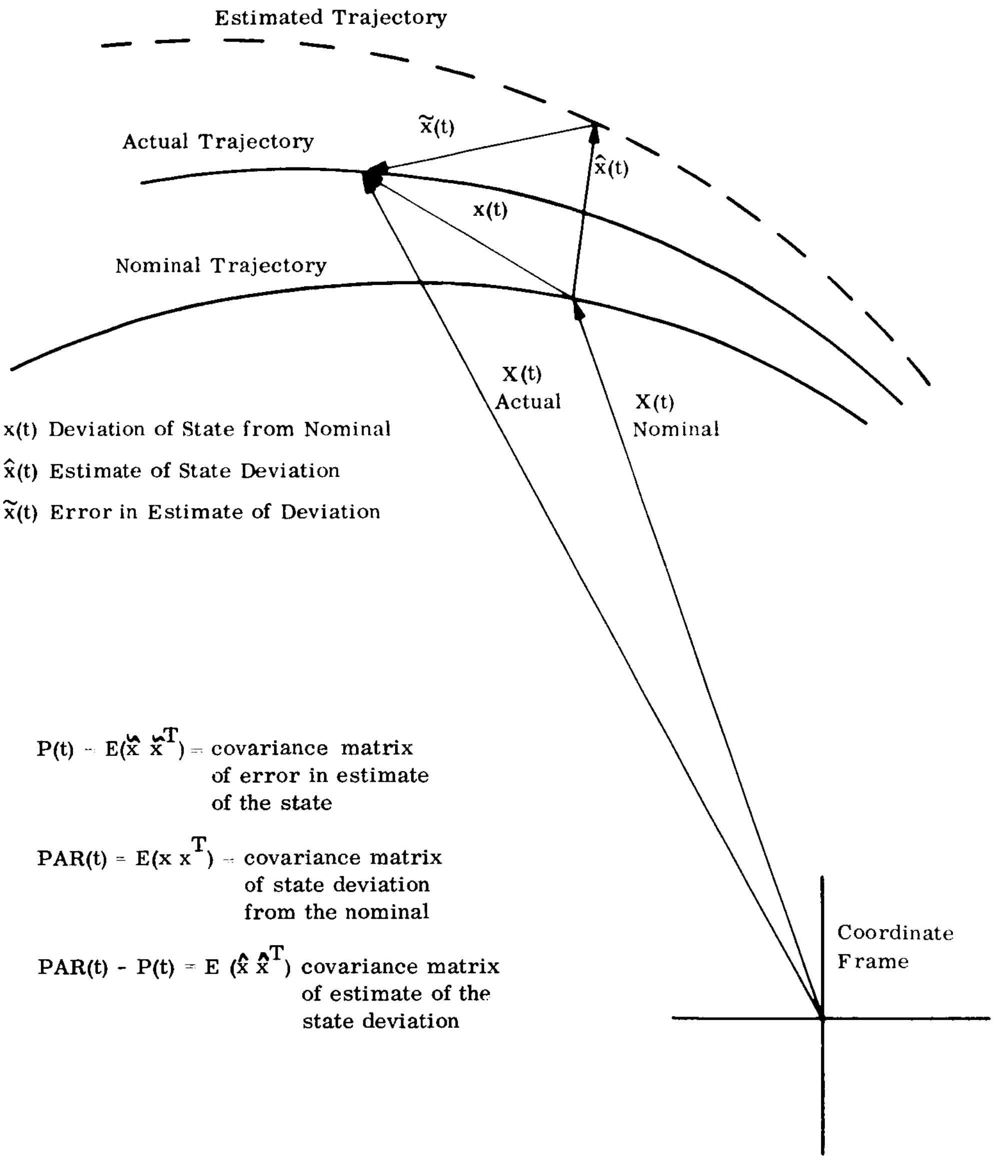

x(t) Deviation of State from Nominal

$\hat{x}(t)$ Estimate of State Deviation

$\tilde{x}(t)$ Error in Estimate of Deviation

$P(t) = E(\tilde{x}\,\tilde{x}^T) =$ covariance matrix of error in estimate of the state

$PAR(t) = E(x\,x^T) =$ covariance matrix of state deviation from the nominal

$PAR(t) - P(t) = E\,(\hat{x}\,\hat{x}^T)$ covariance matrix of estimate of the state deviation

Figure 2-1 State Deviations

GUIDANCE AND NAVIGATION ERROR DATA

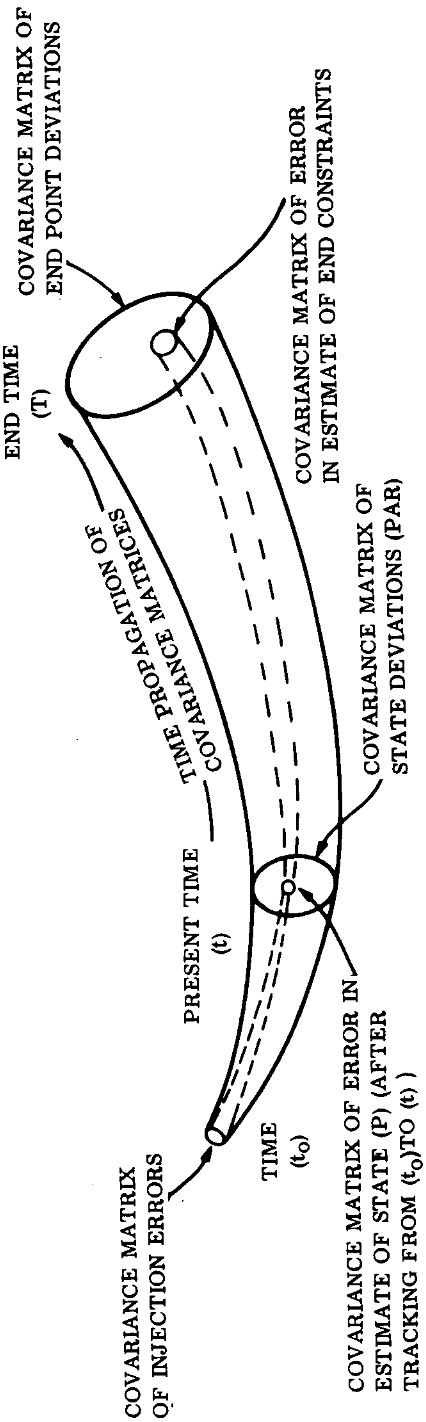

Figure 2-2A

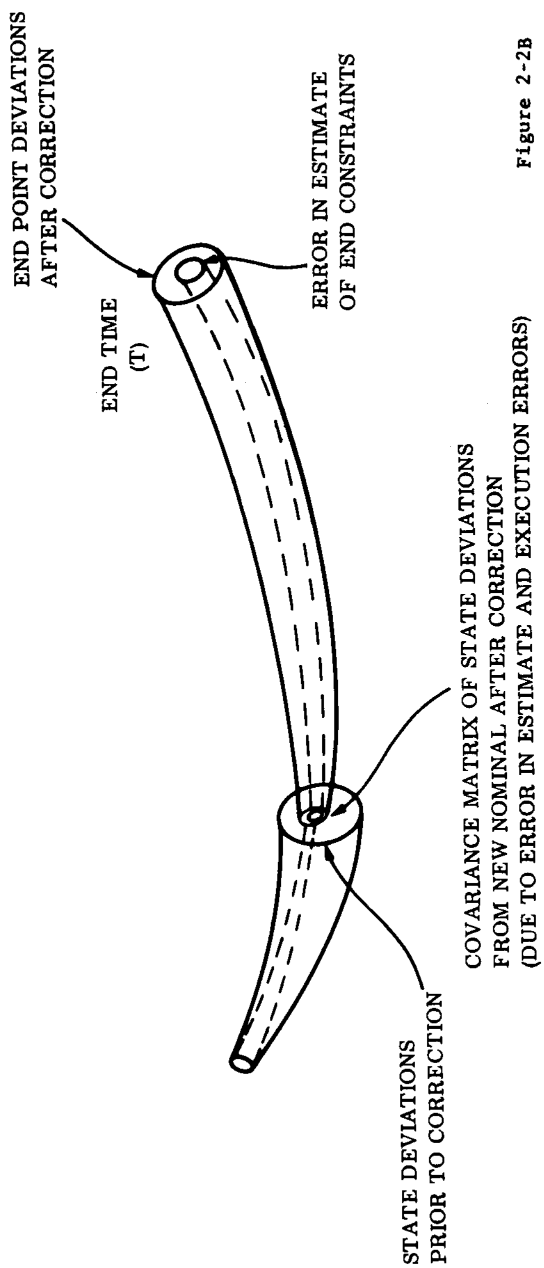

Figure 2-2B

Figure 2-2 Guidance Data After a Correction

Fixed Time of Arrival (FTA)

$$\left[\dot{X}g\ (t) = -D_2^{-1}\begin{pmatrix}\Delta x\\ \Delta y\\ \Delta z\end{pmatrix}\right]_T$$

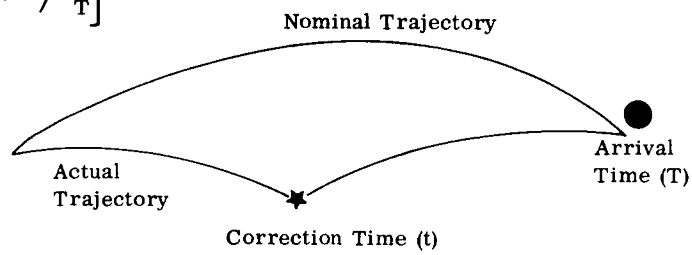

Variable Time of Arrival (VTA)
Velocity Relative to Target Constraint

$$\left[\dot{X}g\ (t) = -D_2^{-1}\begin{pmatrix}\Delta B\bullet T\\ \Delta B\bullet R\\ \Delta V_\infty\end{pmatrix}\right]_{T+\Delta T}$$

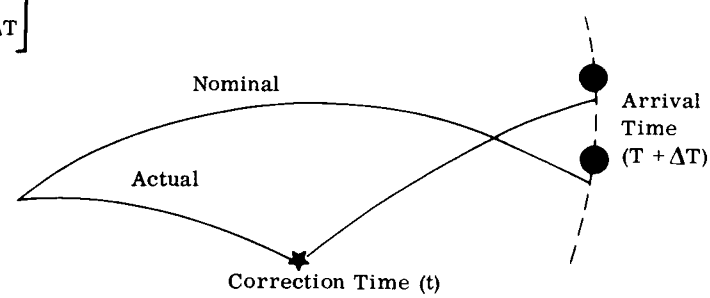

Variable Time of Arrival (VTA)
Minimize ΔV Constraint

$$\left[\dot{X}g\ (t) = -D_2^{-1}\begin{pmatrix}\Delta B\bullet T\\ \Delta B\bullet R\\ \Delta M\end{pmatrix}\right]_{T+\Delta T}$$

ΔM Selected to Minimize ΔV Required

$\dot{X}g$ = Guidance Correction

D_2 = Matrix of Sensitivities Relating Constraints at (T) to Velocity Changes at (t).

Figure 2-3 Guidance Laws

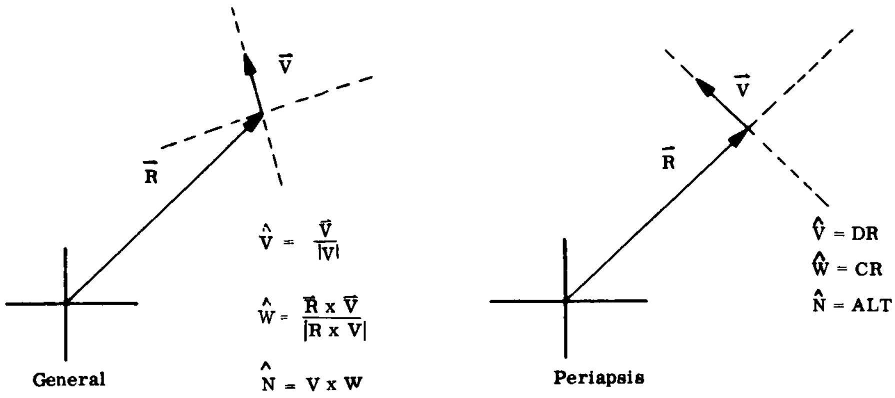

Figure 2-4A NVW Coordinates

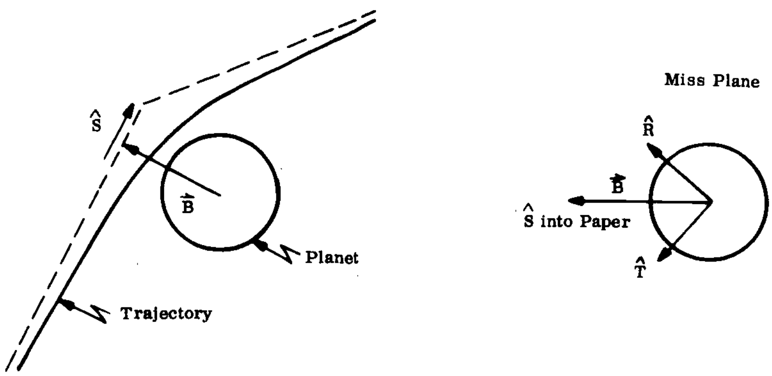

Figure 2-4B B Vector Coordinates

SECTION 3

DESCRIPTION OF DIGITAL COMPUTER SIMULATION

In order to accomplish the objectives of this study it is necessary to develop a digital computer program which has the capability of simulating both the navigation and guidance systems for an interplanetary mission. The Conic Error Propagation Program (CEPP) used in this study has the following features:

1) Patch-Conic Nominal Trajectory

2) Closed-Form Analytic Expressions for the Transition Matrix

3) Navigation Capability

   a. Earth-Based Measurements (Range, Range-Rate, Azimuth, Elevation)

   b. Onboard Measurements (Radar,Range, Range-Rate, Theodolite, Sextant, Subtended Angle Range)

   c. Kalman Filter used to smooth observation data.

4) Guidance Capability

   a. Guidance Law (FTA, VTA with v_∞ constraints, VTA with ΔV minimized)

   b. Parametric Analysis of Error Sources (Pointing, Resolution, Proportional Errors).

SECTION 4

ONBOARD MEASUREMENT TECHNIQUES

The overall function of the navigation system, as defined in this study, is to determine the best estimate the vehicle's position and velocity. An important part of this estimation process for an onboard system is the selection of an observation schedule using a sextant or theodolite. Three types of auxiliary data which are useful in selection of a schedule are presented. The data concern measurement accuracy, celestial body selection and star selection. This technique of onboard scheduling is treated in more detail in Reference 4.

4.1 BODY SELECTION

The measurement gradient vector H is important because it indicates the direction in the state space in which the estimate is improved by the measurement. The gradient associated with an angular measurement such as a sextant measurement of a star-planet angle (Figure 4-1) is normal to the direction of the line of sight (LOS) and in the plane in which the angle is measured. Two orthogonal sextant measurements (Figure 4-2) or the equivalent two theodolite angle measurements have gradient vectors which span the two dimensional position space normal to the direction of the LOS. The third direction of the position space can be determined most favorably by using a second planet with a LOS direction normal to the first. The accuracy of a single position estimate along one of the H vectors is determined by the instruments measurement error. The standard derivation of the angular measurement error has been assumed to be

$$\sigma_\epsilon = \sqrt{k_1^2 + 4k_2^2 \left(\sin^{-1} \frac{RAD}{|R|}\right)^2} \qquad (4\text{-}1)$$

where

k_1^2 = the variance of the angular error when the instrument is used for star-star measurements

k_2^2 = the variance of the angular error when the instrument is used to measure the subtended angle of the body at some low altitude

RAD = radius of the body

$|R|$ = range to body center

The error model given by (4-1) is based on the assumption that as the body is approached, its size in the field of view increases, which causes a greater error in detecting the apparent center or rim.

Since the measurement error is an angular error, the position uncertainty established with such a device is directly related to the range of the body being observed. The uncertainty in a position measurement ϵ_p as a function of range to the center of the planet of interest, is given by

$$\epsilon_p = \sigma_\epsilon |R|$$

$$|R| = \text{Range to planet} \tag{4-2}$$

$$\sigma_\epsilon = \text{Measurement error (standard deviation)}$$

The error in position for a single observation of various planets on the outbound trajectory is shown in Figure (4-3A). The data in Figure (4-3B) are the right ascensions of the celestial bodies in a vehicle centered ecliptic coordinate frame. Since the interplanetary trajectory is nearly in the ecliptic plane, these data can be used to select bodies which have orientation (ideally orthogonal) such that the two dimension inplane position can be estimated. The position coordinate normal to the ecliptic can be estimated by using any of the bodies and a background star in the direction normal to the ecliptic plane.

The out of plane observations should therefore be confined to using the one body which provides the most accurate measurement.

The problem of determining the two dimensional position in the trajectory plane is more difficult since it is necessary to select two bodies whose measurement H vectors span the trajectory plane. The selection of a schedule for inplane measurements is made on the basis of the location of the bodies in the ecliptic plane relative to the vehicle as well as the measurement accuracy data.

Figure 4-3A indicates that for the early part of the trajectory, the Earth provides the best measurement accuracy. The Moon would also provide good navigation data at this time. Although from Figure 4-3A the Sun appears to provide fairly good measurement data, the use of this body would not be expected to provide any additional information for the first 40 days. This is because the RA of the Earth and the RA of the Sun in the early part of the trajectory are almost 180° apart and therefore, the position information obtained from these two bodies is almost colinear. Figure 4-4, which shows the propagation of injection errors and includes the effects of Earth and Sun observations made along the outbound trajectory, shows that there is, in fact, a degradiation performance by replacing some of the Earth observations with Sun observations, rather than using just Earth observations. The figure also indicates no change in the $\vec{B} \cdot \hat{T}$ error and implies, therefore, that this constraint is dependent on the coordinate which is normal to that determined by either the Earth or the Sun.

In order to obtain a good position estimate along the direction normal to the position estimate provided by the Earth, it is necessary to use a body whose RA is about 90° from that of the Earth. The approximate value of this RA is defined by A-A Figure 4-3B. Any body whose RA passes through the cross hatch area will provide good information on the coordinate normal to the A-A for the first 60 days. At twelve hours from injection the Moon passes through the area as shown by the figure. During this time it is possible to obtain a good measurement of the coordinate normal to A-A, since the measurement accuracy using the Moon at this time is good as seen in Figure 4-3A.

The value of Moon observations at this time is verified by Figure 4-5 which shows a reduction in the $\vec{B}\cdot\hat{T}$ error in estimate starting at about 5 hours from injection.

An alternate method for obtaining information on the coordinate normal to A-A is to make Sun observations starting at 40 days. At this time the Sun crosses the region of interest in Figure 4-3B and takes 40 days to cross it. The tracking data shown in Figure 4-6, which uses Sun and Earth observations during the first 100 days, shows that the Sun observations at about 40 days have the same effect as the Moon in reducing $\vec{B}\cdot\hat{T}$ error in estimate.

The number of observations taken is important because each observation requires a certain amount of time and fuel to maneuver the vehicle into the proper attitude. It is therefore, desirable to adopt a schedule where the number of observations is not excessive. One of the main considerations in determining the number of observations is the accuracy of the measurement. During the early part of the midcourse trajectory the Earth provides accurate measurements and near the end Mars provides accurate measurements. Also at these times there is only one body to observe and therefore maneuvering is held to a minimum.

The number of observations is also important, because there is a trade-off between instrument accuracy and the number of observations. This is shown in Figure 4-7, where the navigation performance is compared for two sextants with accuracies of 10 arc-and 20 arc-seconds. Curves (1) and (2) have been obtained with 162 inplane measurements and 32 out of plane measurements. The degradation in performance with the 20 arc-second device at 220 days is 100%. This is the type of increase that would be expected in a linear system where a parameter is estimated with an instrument having only random errors.

The results in curve (3) shows that the error in estimate is reduced very nearly by the square root of the number of observations $\left(\sigma_{EST} = \frac{\sigma_{INST}}{\sqrt{N}}\right)$.

This curve (3) represents the results obtained for a 20 arc-second device and four times as many observations as in the other two cases. As seen from the figure, the estimation for curve (3) is almost identical as that for the more accurate instrument.

4.2 STAR SELECTION

In order to determine the availability of specific stars for use with a sextant along the trajectory, that can also be used in conjunction with the body selection schedule, the right ascension of Earth, Mars and the Sun, in a vehicle centered 1950 equator of data coordinate system is shown in Figure 4-8A. Figure 4-8B, shows the celestial sphere as seen from the spacecraft where the dotted lines are the ecliptic plane projected onto the sphere, and some of the first, second and third magnitude stars near the ecliptic have been included. The feasibility of taking a sextant measurement at a given time can be determined by first selecting a body from the body selection schedule, and then using Figure 4-8A and Figure 4-8B to determine whether the availability of stars and the position of the Sun will make the observation possible.

The data in Figure 4-8A can also be used to evaluate the position of the Sun relative to a body of interest. This would be done to ensure that the Sun did not "blind" the instrument being used. For example, at the time of 120 days the Earth is fifty degrees away from the Sun. The figure also indicates that this is as close as the Earth gets to the Sun along the whole trajectory.

In order to illustrate the use of Figure 4-8, an example is now considered. Assuming the body selection data indicates that the observations of the Sun and Earth are desirable at 120 days, Figure 4-8A is entered at this time. As shown by the dotted lines, the right ascensions of these bodies are projected into the ecliptic plane shown on the celestial sphere in Figure 4-8B.

The intersection of the dotted lines and the ecliptic plane represents the positions of the Sun and Earth on the celestial sphere as viewed from the spacecraft at 120 days along the trajectory. Forty by sixty degree sectors about each of these points have been enlarged and are shown in Figure 4-9. Overlayed on each section is a twenty degree diameter circular window. The overlay could be made to any size and shape which corresponds to the vehicle's observations window constraints. The vehicle windows shown in the figure present the bodies of interest and the background stars available at the specified time.

The upper part of Figure 4-9 shows that the first magnitude star, Regulus, can be used for a measurement of the position in the $\hat{u}$ direction. The use of the star would be restricted to a slightly earlier or later time since it is directly in the Sun at the time shown. The time difference which would be required would depend on the angular separation between a star and the Sun required for making such a measurement when using a specific instrument. Slightly earlier in the flight (3 degrees right ascension or about 4 days), the third magnitude star γ_{LEO}, in the upper part of the window would be in an ideal position for a measurement in the $\hat{t}$ direction. The same type of analysis can be performed to select suitable stars for use with the Earth as a reference body. This is shown in the lower portion of Figure 4-9. In this case the star, Spica, could be used for a $\hat{t}$ measurement and a few days later it would be positioned for a measurement in the $\hat{u}$ direction.

If these two bodies, Sun and Earth were to be observed at approximately the same time, Figure 4-8 also indicates that the vehicle must be reoriented fifty two degrees in RA and twenty degrees DEC. With a specific control system, these required excursions could be used to generate data on the time and fuel requirements for such a maneuver.

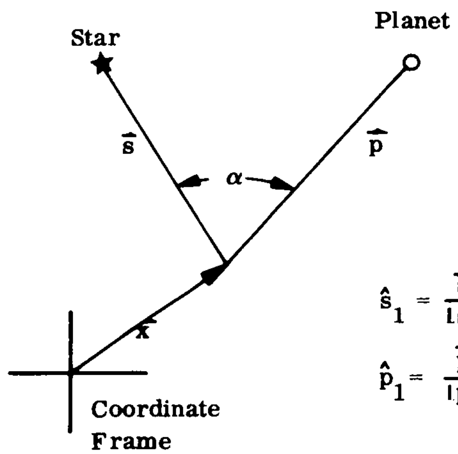

$$\hat{s}_1 = \frac{\vec{s}}{|s|}$$

$$\hat{p}_1 = \frac{\vec{p}}{|p|}$$

$$\cos\alpha = \hat{s}_1 \bullet \hat{p}_1 = \hat{s}_1^{\,T} \hat{p}_1$$

$$\nabla_x \alpha = -\frac{1}{\sin\alpha} \left(\hat{s}_1^{\,T} \nabla \hat{p}_1 + \hat{p}_1^{\,T} \nabla \hat{s}_1 \right)$$

$$\nabla_x \alpha = \frac{\hat{s}_1^{\,T}}{|p| \sin\alpha} \left(I - \hat{p}_1 \hat{p}_1^{\,T} \right)$$

$$= \frac{1}{|p|} \left\{ \frac{\hat{p}_1 \times \hat{s}_1}{|\hat{p}_1 \times \hat{s}_1|} \times \hat{p}_1 \right\}$$

Figure 4-1 Gradient of Sextant Measurement

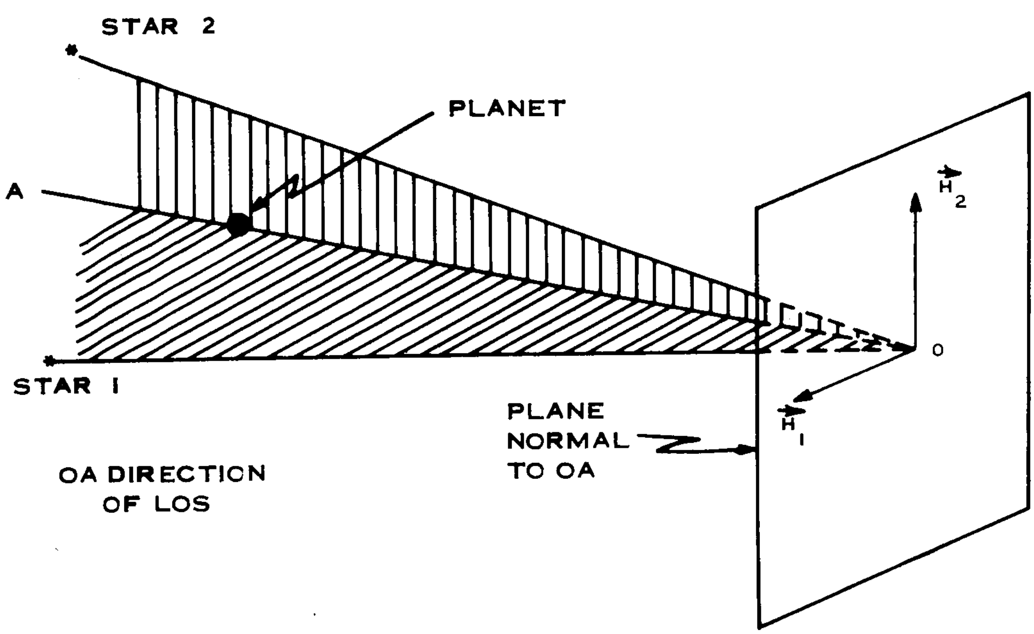

Figure 4-2 Problem of Determining the Two Dimensional Position in the Trajectory Plane

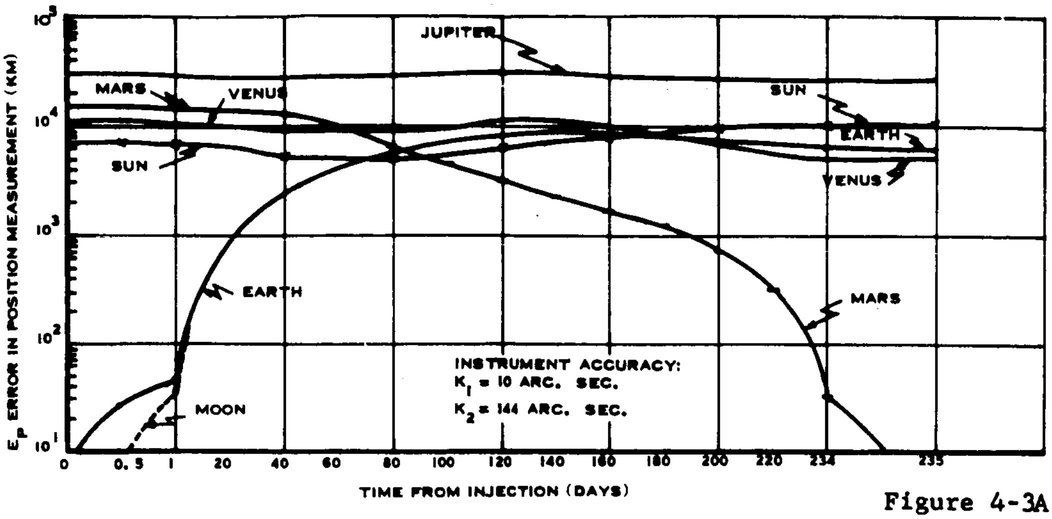

Figure 4-3A

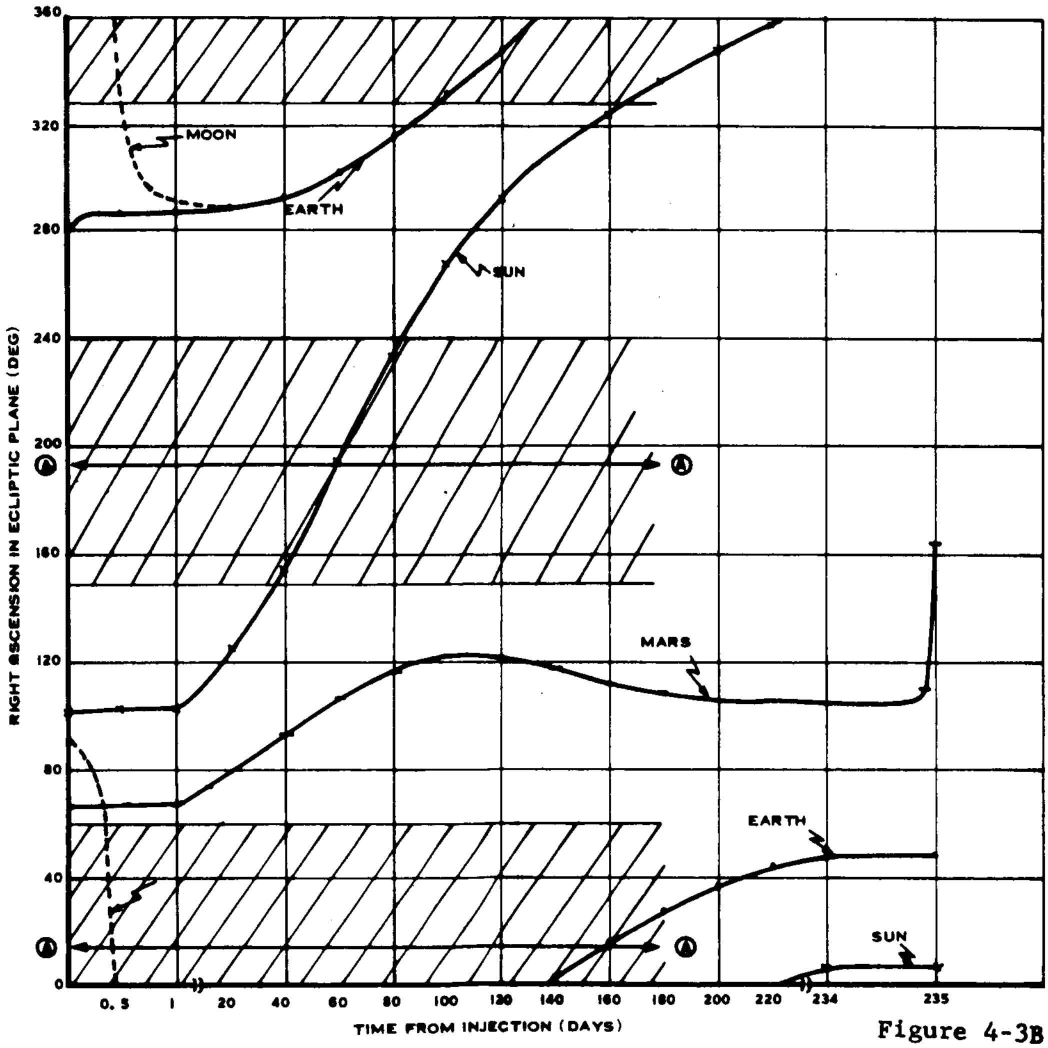

Figure 4-3B

Figure 4-3 Schedule Data for Earth-Mars Trajectory

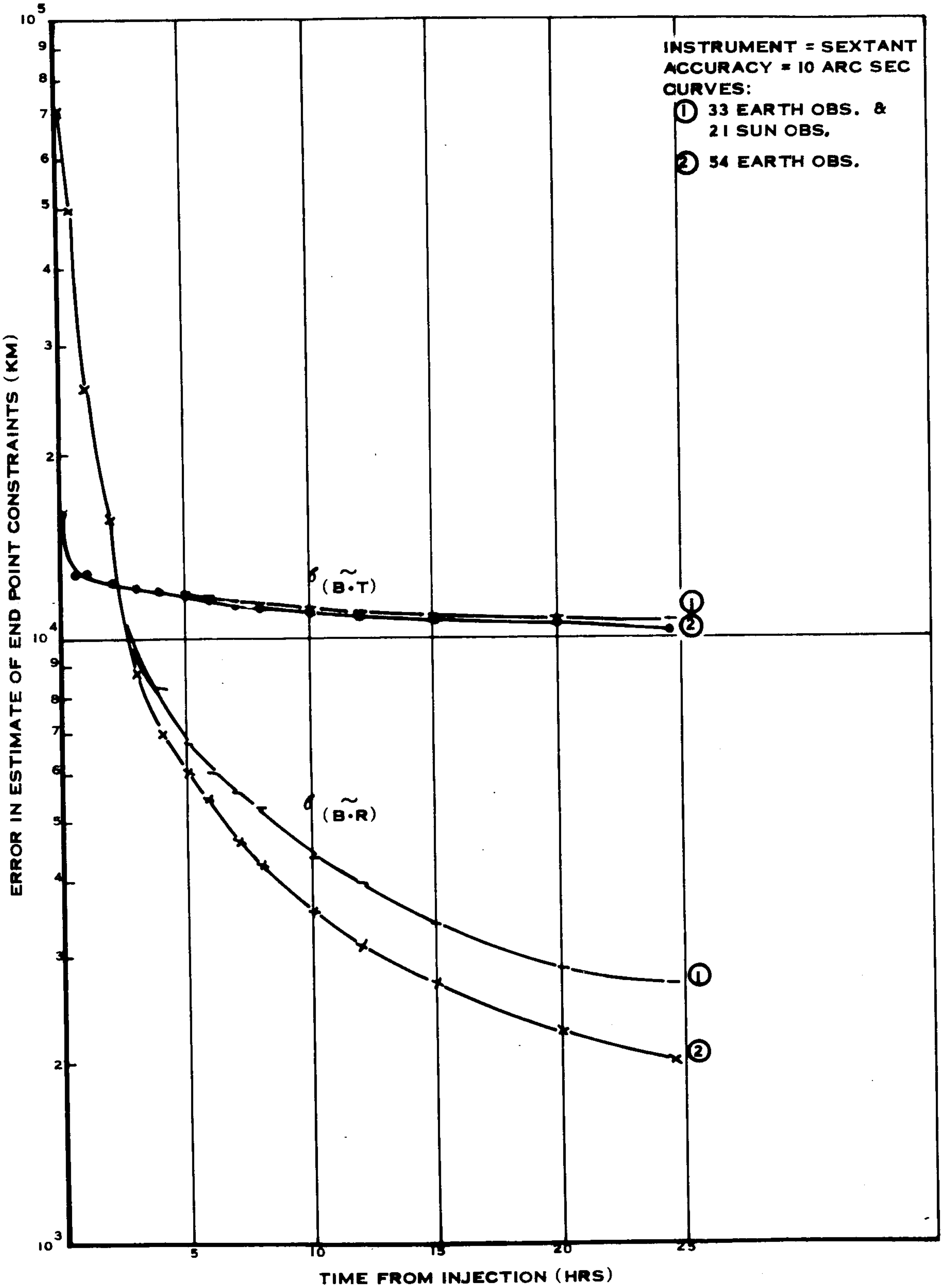

Figure 4-4 Influence of Using Sun Observations Early on the Earth-Mars Trajectory

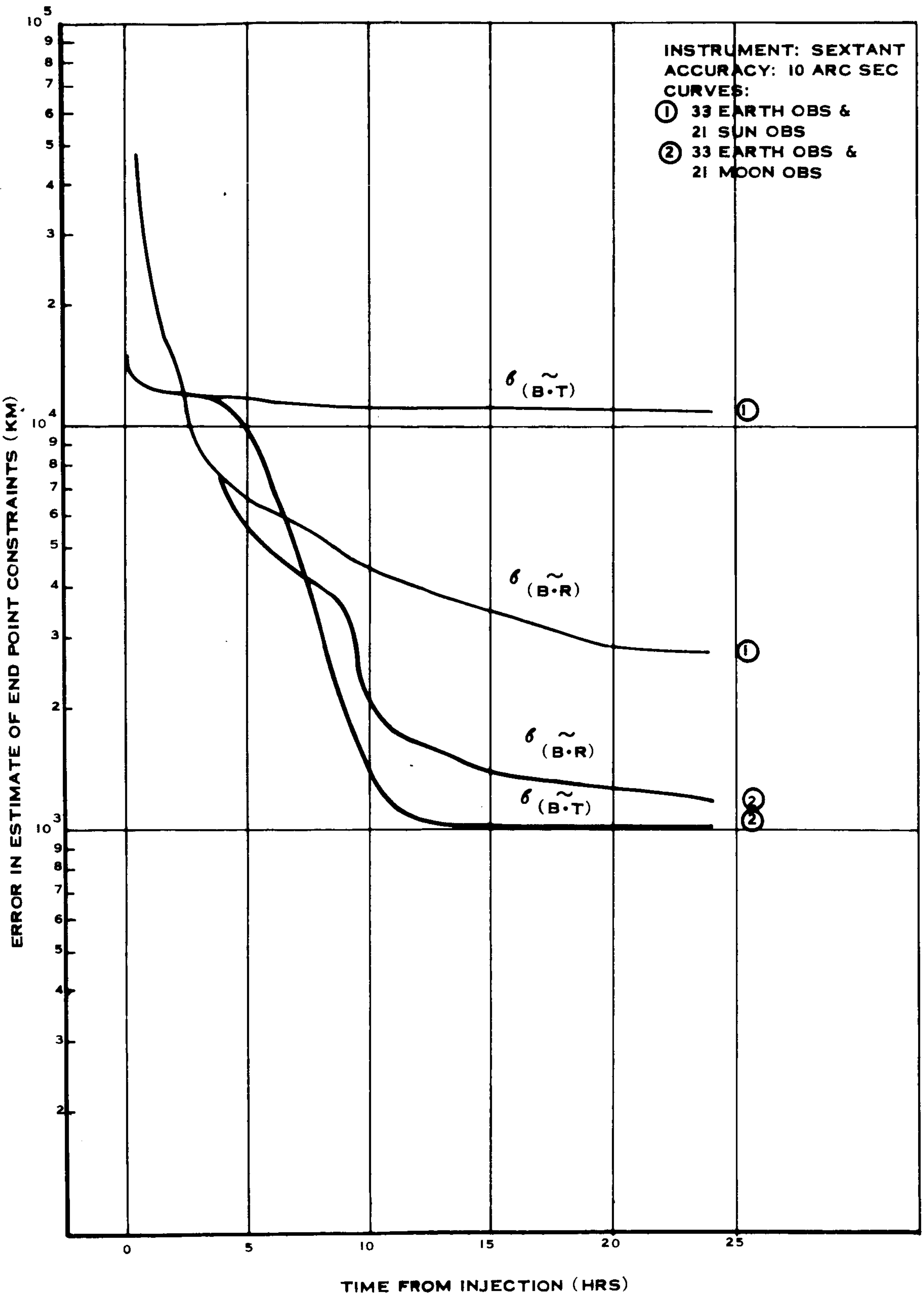

Figure 4-5 Influence of Using Moon Observations on the Earth-Mars Trajectory

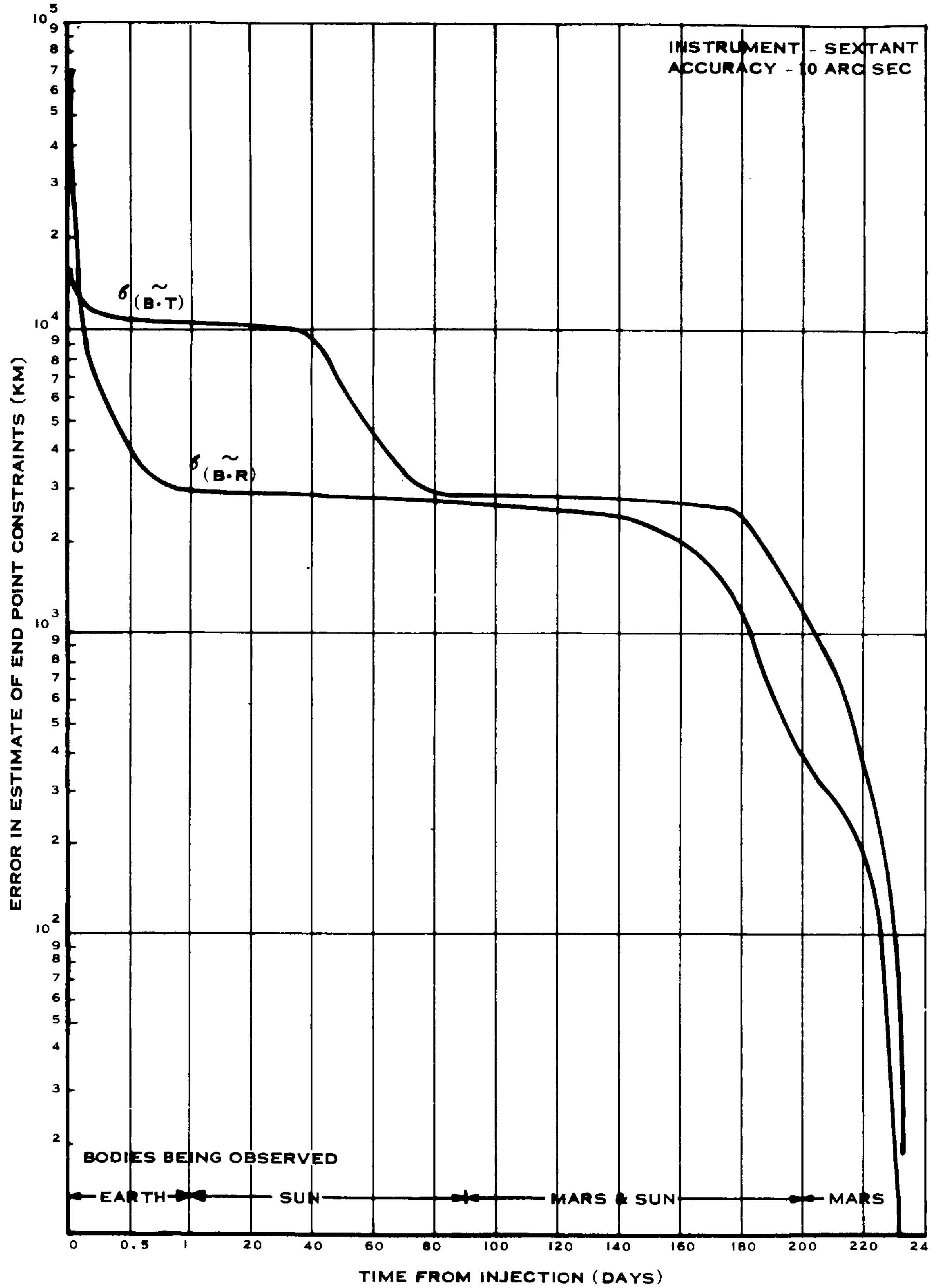

Figure 4-6 Tracking Data for Earth-Mars Trajectory

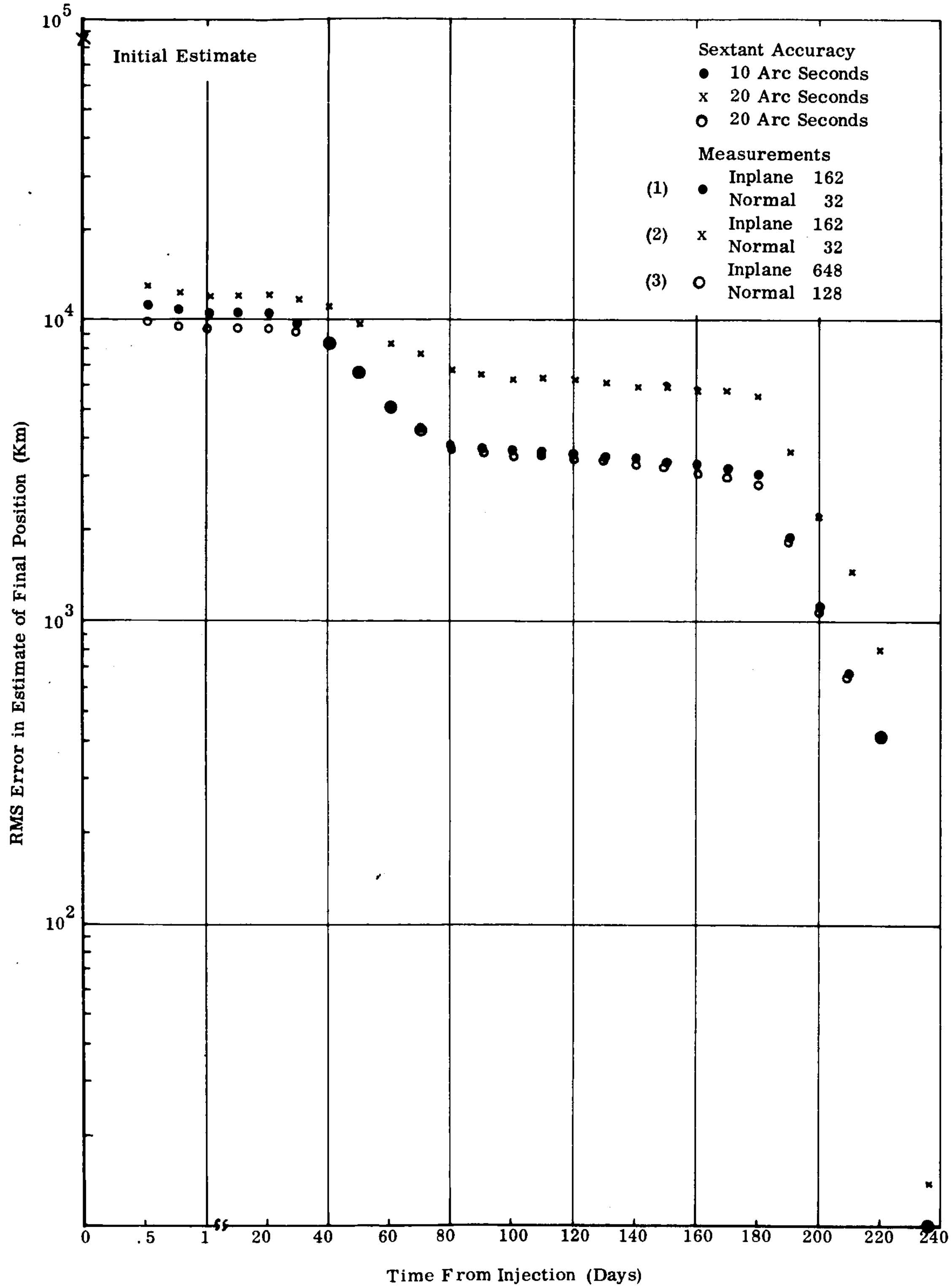

Figure 4-7 Tradeoff Between Instrument Accuracy and Number of Observations

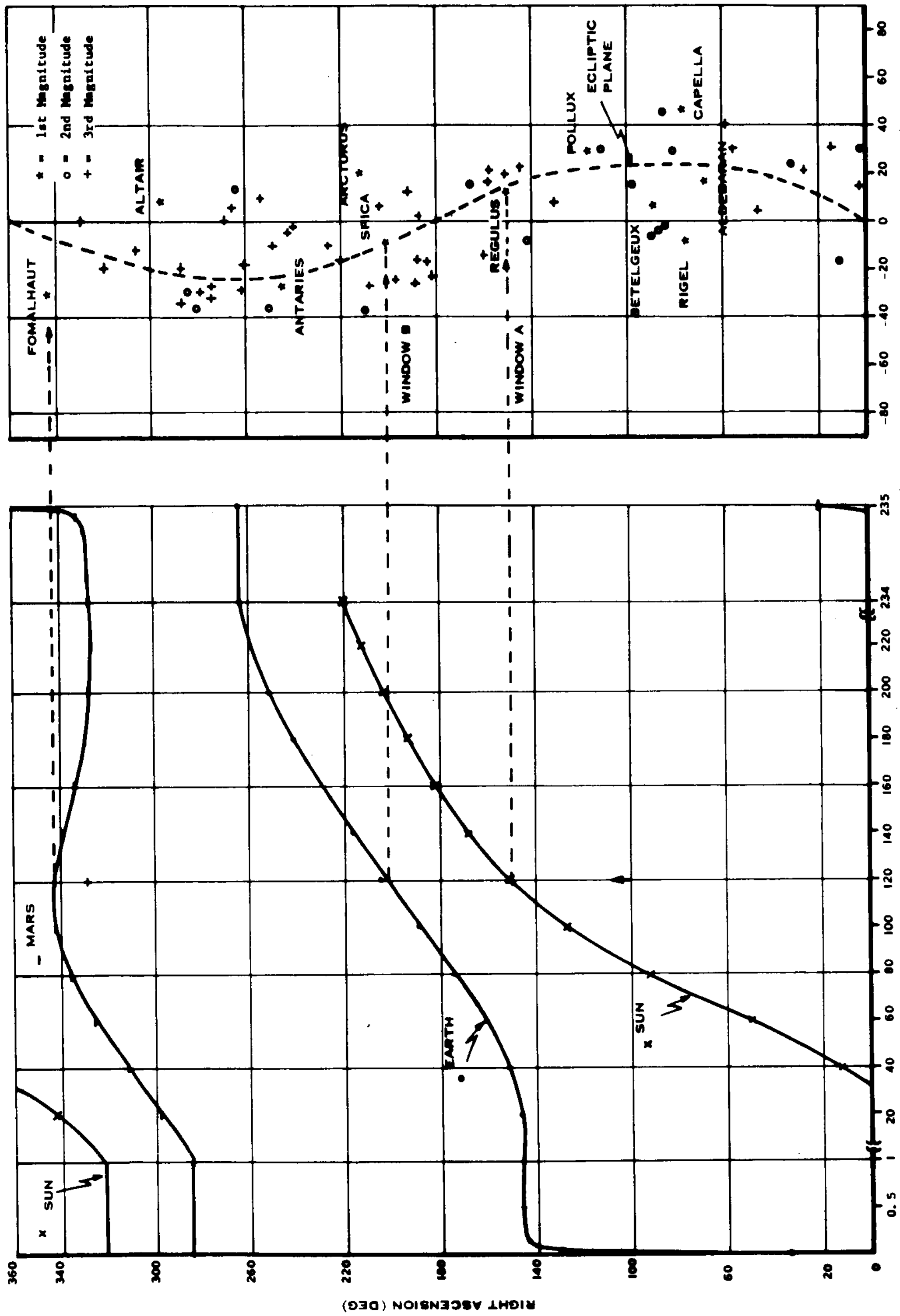

Figure 4-8B

Figure 4-8A

Figure 4-8 Star Selection Data

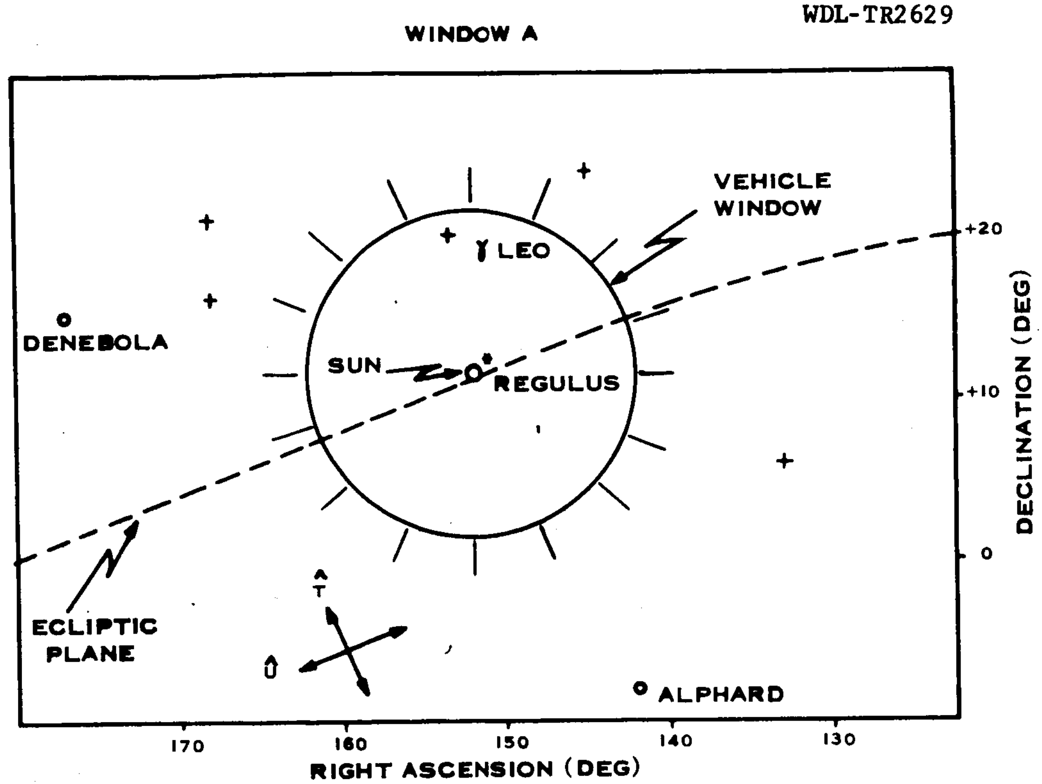

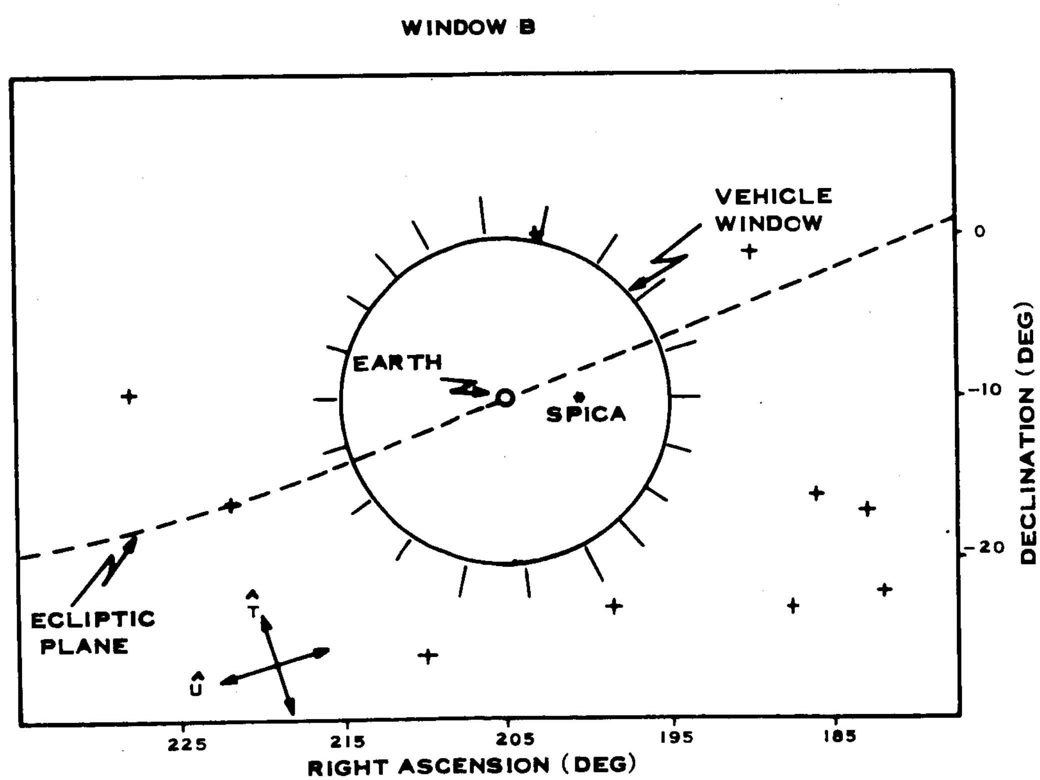

Figure 4-9 Vehicle Observation Windows

SECTION 5

EARTH MARS MIDCOURSE ANALYSIS

The principal results of this study, which include a statistical error analysis of the navigation and guidance system, are summarized in Sections 5, 6, and 7. The analysis in this section pertains to the midcourse phase of the Earth-Mars mission. It is defined to be the interval of time between injection onto the transfer trajectory from a 185 km altitude Earth park orbit and the point of closest approach to Mars. Since it has been found that the accuracy of the guidance system is highly dependent on the accuracy of the navigation system, the navigation is studied first and these results are then used to study the guidance system.

The analysis of the navigation system is concerned with determining the accuracy with which the position and velocity of the vehicle can be estimated. Since one of the primary objectives of the study is to compare the capabilities of groundbased and onboard navigation systems, the navigation analysis is carried out for each of the four systems described in Section 1. The overall figure of merit that is used for comparing the navigation systems is the error in estimate of the end-point constraints on the nominal trajectory.

The guidance analysis for the midcourse phase is concerned with determining the number of corrections and times at which they are made, evaluating two different guidance laws, and analyzing the effects of errors resulting from the thrusting maneuvers. The figure of merit used for evaluating the guidance system is the deviations of the end-point constraints. The specific deviation requirements depend to a large extent on the mission itself. For example, with Mariner IV, the primary concern was to flyby the planet with a high probability of not impacting. With the large value of radius of closest approach that was used, large guidance deviations could not be tolerated. If instead an atmospheric braking maneuver were to be executed at Mars, a much smaller tolerance on the deviations is required.

In the analysis of the four systems which follows, a basis of comparison which is used is a $\pm$ 3.5 km deviation in the altitude direction. This would be sufficient guidance accuracy for the terminal maneuver to be performed with atmospheric maneuvering. This deviation error represents approximately a three-sigma confidence level of hitting a 21 km entry corridor at Mars. This corridor width was obtained in a previous study.*

The analysis in this section has been performed for a given nominal trajectory and for assumed numerical values of the statistical errors. Use of the results in this section to specify hardware requirements is therefore limited by these assumptions that have been made for the Earth-Mars mission. However, the techniques that have been developed to analyze the guidance and navigation requirements are not limited, and in fact, could be applied to any interplanetary mission.

5.1 NAVIGATION SYSTEM COMPARISON

In this section the navigation performance is measured by the error in $\vec{B}\cdot\hat{T}$ and $\vec{B}\cdot\hat{R}$ end-points estimates for each of the four systems defined in Section 1. Although bias errors clearly affect the error in estimate of the state, with the exception of station-location bias errors, only unbiased statistical measurement errors are considered.

The effect of the station-location bias errors on the performance of System I is shown in Figure 5-1 by considering three different cases. First, neglecting the bias errors yields a terminal error in estimate of approximately 100 km.** Second, including the effects of 100 meter station-location bias errors in both the north and east directions causes the error in estimate to increase to approximately 250 km. In the third case errors have been included as part of an expanded state vector and the numerical values of these errors has been determined.

* The study of parameters and the definition of the corridor bounds are described in Reference (5).

** On the low energy trajectory the error in estimate is 25 km.

The estimation of the bias error reduced the end-point estimate to 120 km. The decrease in the error in estimate of the location of the Johanesburg tracker is shown in Figure 5-2. The errors in the north and east location are reduced from 100 meters to approximately 10 meters. These data indicate that by using parameter estimation techniques[6] for the bias error sources it is possible to reduce the magnitudes of these uncertainties. In fact, if as a result of using this technique, the bias error uncertainties are removed, then the data obtained which have neglected bias errors, become quite realistic.

The navigation data for the four system configurations is shown in Figure 5-3. The onboard instrument is a 10 arc-second theodolite. The type of mission which these systems are capable of can be inferred from these data. The use of the DSIF (System I) provides a relatively good estimate of the end constraints early in the flight compared to System IV, the onboard system. It has an accuracy limited to approximately 100 km. The addition of the onboard tracker (System II and III) provides in improvement in the terminal accuracy of approximately two orders of magnitude. System IV provides terminal accuracies of the same order as II and III. The poorer estimates during the early phase of the trajectory resulted in slightly larger velocity requirements. This is due to the first correction being made with a larger error in estimate of the end constraints.

Figures 5-4 and 5-5 summarizes the navigation and guidance performance of the four system configurations as a function of the onboard instrument accuracy. The guidance system used to obtain these guidance data is a nominal "state of the art" system.* The $\vec{B}\cdot\hat{T}$ data in Figure 5-4 indicates the capabilities of the systems to estimate and control the distance of closest approach with VTA guidance law. It indicates the instrument accuracy required under the assumptions made, to hit an entry corridor with each system configuration.

---

* The nominal guidance system assumes proportional, pointing and resolution errors of 1%, 0.5 degrees, and .1 m/sec, respectively.

System I does not have the capability of such a mission and II, III and IV require instrument accuracies of 12, 18 and 4 arc-seconds respectively. The $\vec{B}\cdot\hat{R}$ data shown in Figure 5-5 corresponds primarily to cross-range errors or uncertainties in the inclination of the apparent trajectory.

A comparison of the guidance deviation and the error in estimate data indicates that with the number of guidance corrections used, the nominal system is capable of controlling the trajectory to within 10-20% of the error in estimate of the constraints. The velocity requirements shown are primarily determined by the size of the injection errors which are used.

5.2 GUIDANCE ANALYSIS

In order to compare the performance of the four navigation systems in the previous section, a guidance system was assumed that consisted of a nominal set of execution errors, and used a particular time schedule for making midcourse maneuvers. In this section, parametric data is presented on the guidance system error sources. Also the type of data used to select the number of guidance corrections as well as the times at which the corrections are made, is discussed.

The first correction data for System I using a VTA guidance law are shown in Figure 5-6. The RMS error in the estimate of the end-point position constraints shown in the figure represent the performance of the navigation system being used. The two curves which show the RMS ΔV required are for the VTA guidance laws which have as $\vec{B}\cdot\hat{T}$ and $\vec{B}\cdot\hat{R}$ two constraints and either the velocity at infinity or a minimum ΔV as a third constraint. The curve of the RMS end-point position deviation after a correction indicates the constraint deviation which would occur if a correction were made at any of the times shown.

The time at which the first guidance correction should be made can be determined from the data in Figure 5-6. An important criteria for selecting a guidance time is the ΔV required and the deviations after the correction.

The two curves in Figure 5-6 indicate that at 2 days the position deviation after a correction is at a minimum and also the required ΔV is low (10.6 m/sec). This first correction primarily compensates for the injection errors. The cause of the magnitude of the end position deviation (1720 km) being considerably larger than the RMS error in estimate (405 km) is the effect of the guidance system execution errors.

The data in Figure 5-6 show that it would be very undesirable to make a correction at 60 days because of the large ΔV requirements. The reason for this large requirement is that the matrix relating changes in the velocity at this time to changes in the end-point constraints becomes singular. This singularity occurs at the time when the true anomaly to the target on the Sun-centered conic is 180° (Figure 1-1). This type of singularity is discussed in Reference 7. Data of this type which shows the required ΔV and the resulting deviations if a correction is made, can also be used to select the number of corrections which should be made. Figure 5-7A shows the results which are achieved for a second correction for System II and III. During the last day, the guidance accuracy reaches a limit of 23 km. This is because the increasing velocity requirements cause the proportional and pointing guidance errors to grow. The error in estimate is reduced to approximately 3 km at this time. Therefore if the number of corrections is limited to two in this case the correction requires approximately a ΔV of 100 m/sec to achieve an accuracy of 23 km or 20 m/sec for 30 km accuracy. The data in Figure 5-7B shows the value of making a third correction. These data assumed a second correction is made 232 days 12 hours which requires a ΔV of 8 m/sec and results in a constraint deviation of 38 km after the correction. The third correction data indicates that with a third correction of 1 or 2 m/second the guidance system can control this trajectory to 4 or 5 km. This is only 20 percent larger than the error in estimate of the constraints. This type of data showed that systems I, II III, and IV required 2, 3, 3, and 4 corrections respectively.

The effects of varying the three guidance system error sources are shown in Figure 5-8 for the system IV navigation system.

The curves shown represent lines of constant end position deviations following the correction. The data show the guidance accuracy after the first correction is dependent on all three error sources. The fourth correction data indicates that if a sufficient number of corrections are made, only the resolution error limits the final accuracy.

When a guidance system is used with the number of corrections restricted, the effects of all the execution errors becomes more important. The parametric error data then permits tradeoffs to be made between the error allotment to each error source in the guidance system. This is illustrated by the data shown in Figure 5-9, which are representative of the effect of guidance system errors on missions where the number of corrections is restricted to one (Mariner IV). The data have been obtained on the nominal trajectory under the assumption that a correction is made at 180 days. The navigation system has been assumed to be perfect.

If the mission objectives required a maximum standard deviation of 2000 km following the correction, the data can be used to define limits on guidance system errors. Fixing the pointing error at .75 degrees, the dotted lines in the figure show two possible limits for the resolution and proportional errors. In one case (Figure 5-9B) if the resolution error is .05 meters/second, the proportional error is restricted to be less than 1.62%. The second case (Figure 5-9C) allows the resolution error to increase to .2 meters/second which then restricts the proportional error to be less than 1.25%.

The data in Figure 5-9A for the case of zero resolution errors shows the maximum allowable errors are 1.05 degrees and 3.0% (extrapolated) for the pointing and proportional error sources respectively, in order to satisfy a deviation of 2000 km. Attitude control and rocket motor subsystems with larger error magnitudes than these could not be considered for the mission which was defined above. The time of correction is another parameter which was not varied but would change the figure as shown and therefore the relationships between the error sources and the error limits.

System IV is used to compare the use of VTA and FTA guidance laws. The performance of the guidance system is very nearly the same (5%) with the two laws. The ΔV requirements with FTA are 56.8 meter/second compared with 23.2 m/second for VTA. This difference is the penalty for controlling arrival time. The arrival time deviation with FTA is 36.0 seconds and with VTA it is 38.6 minutes.

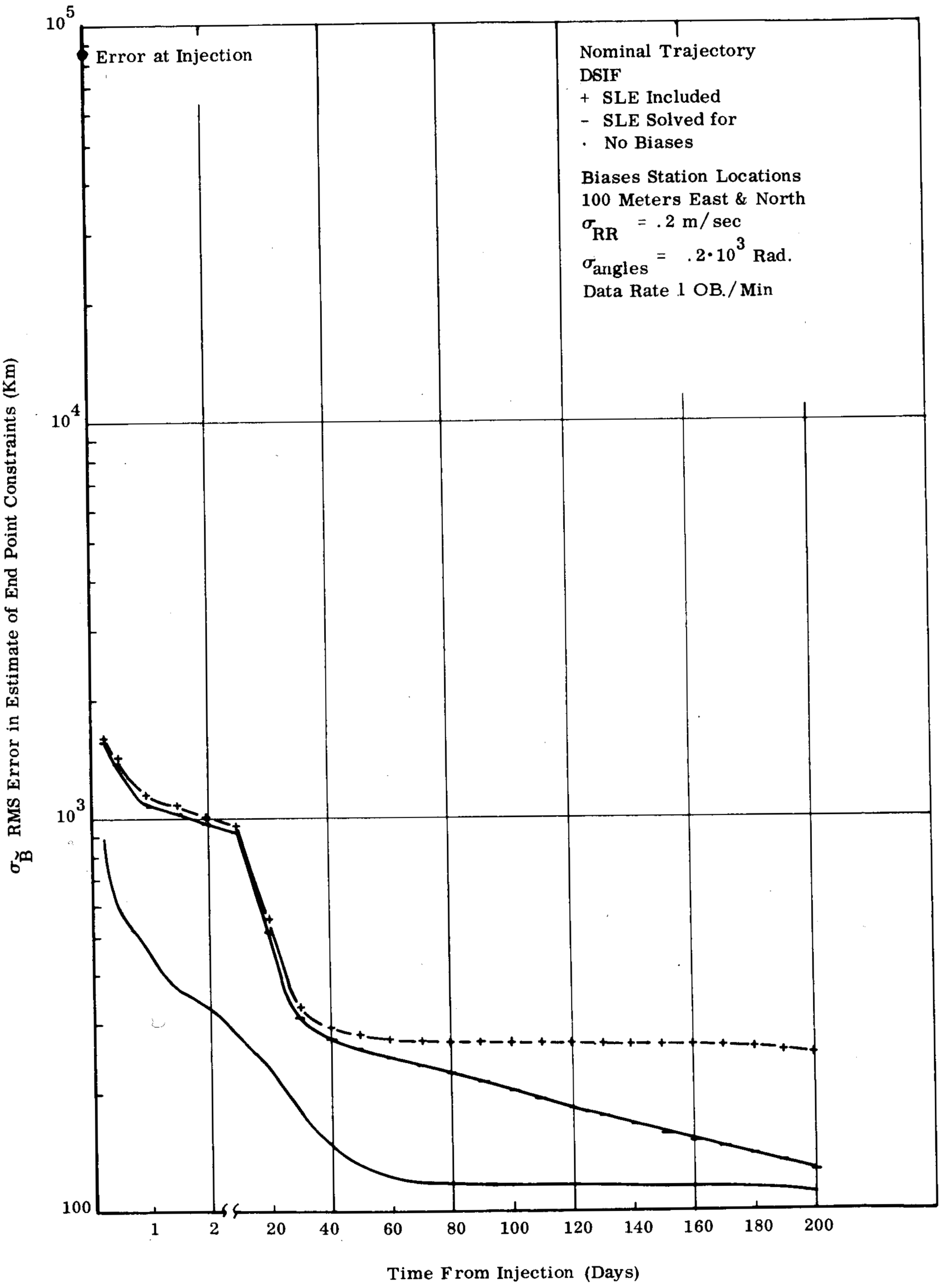

Figure 5-1 DSIF Tracking Data

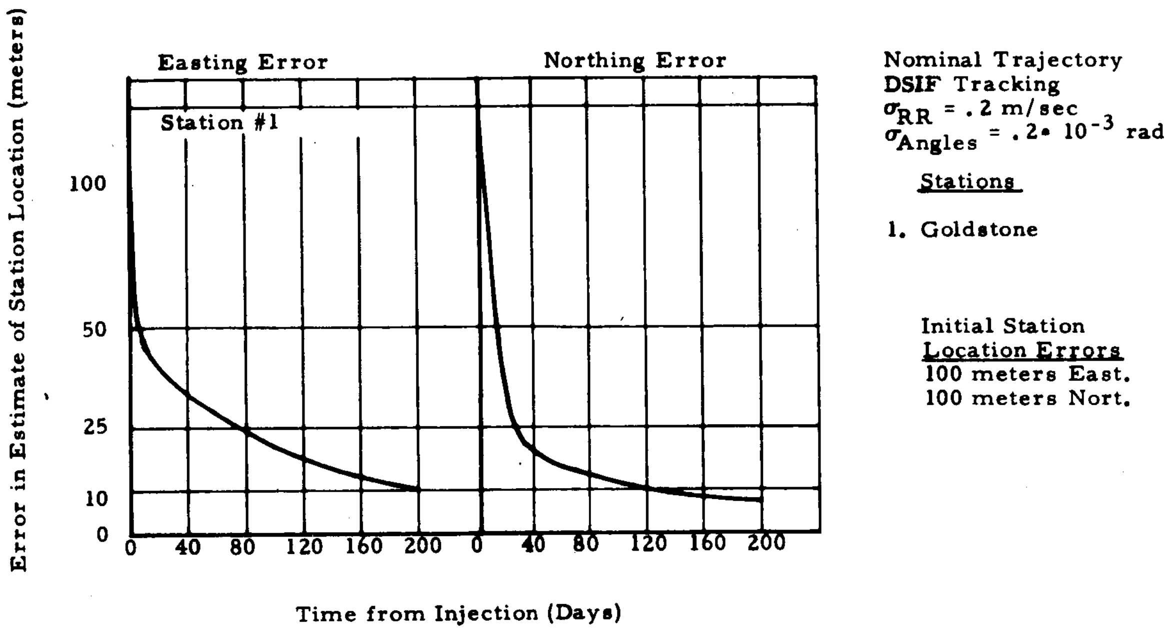

Figure 5-2 Error in Estimate of Station Locations

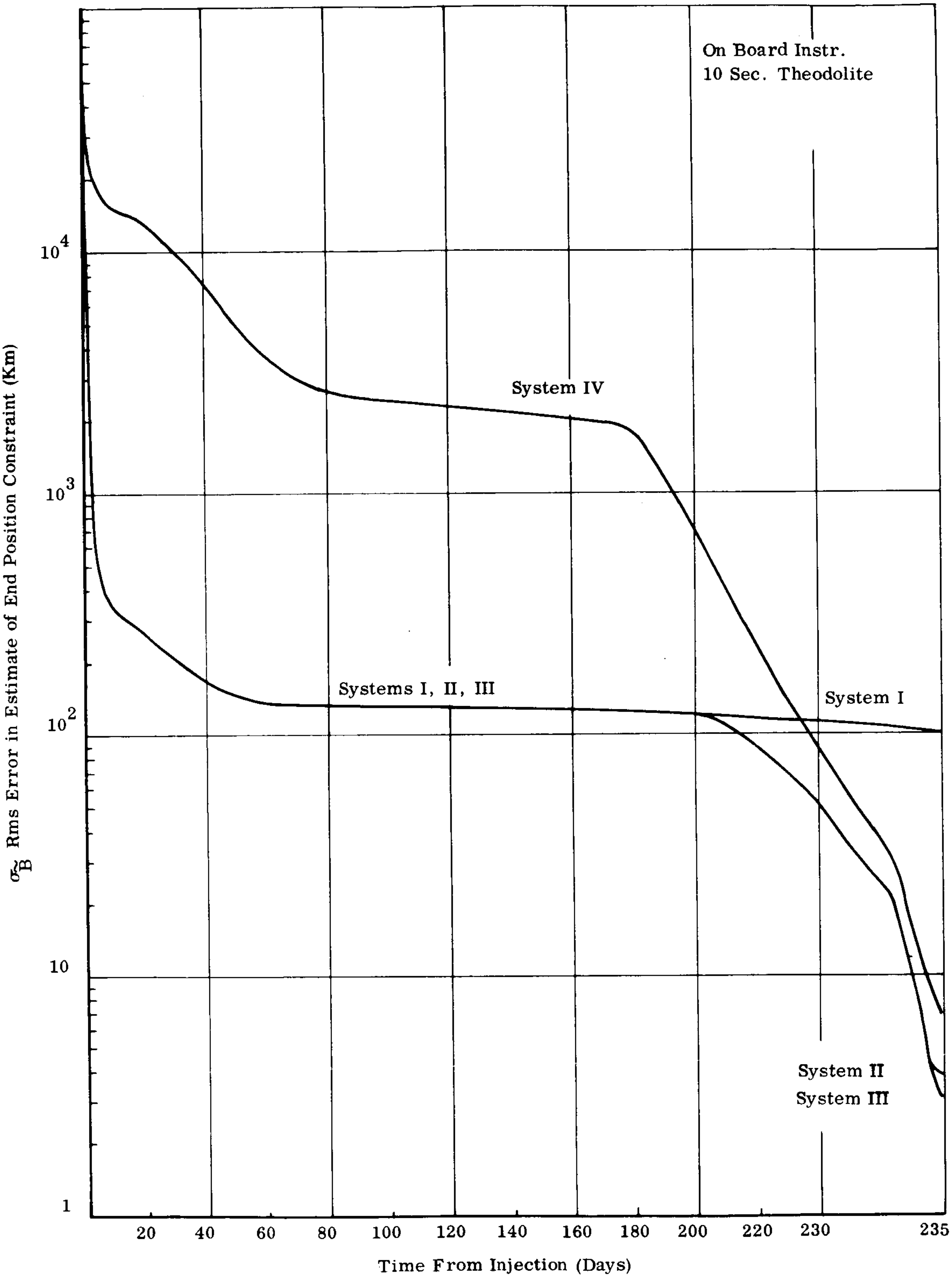

Figure 5-3 Naviation Data for Four Systems
Earth-Mars Trajectory

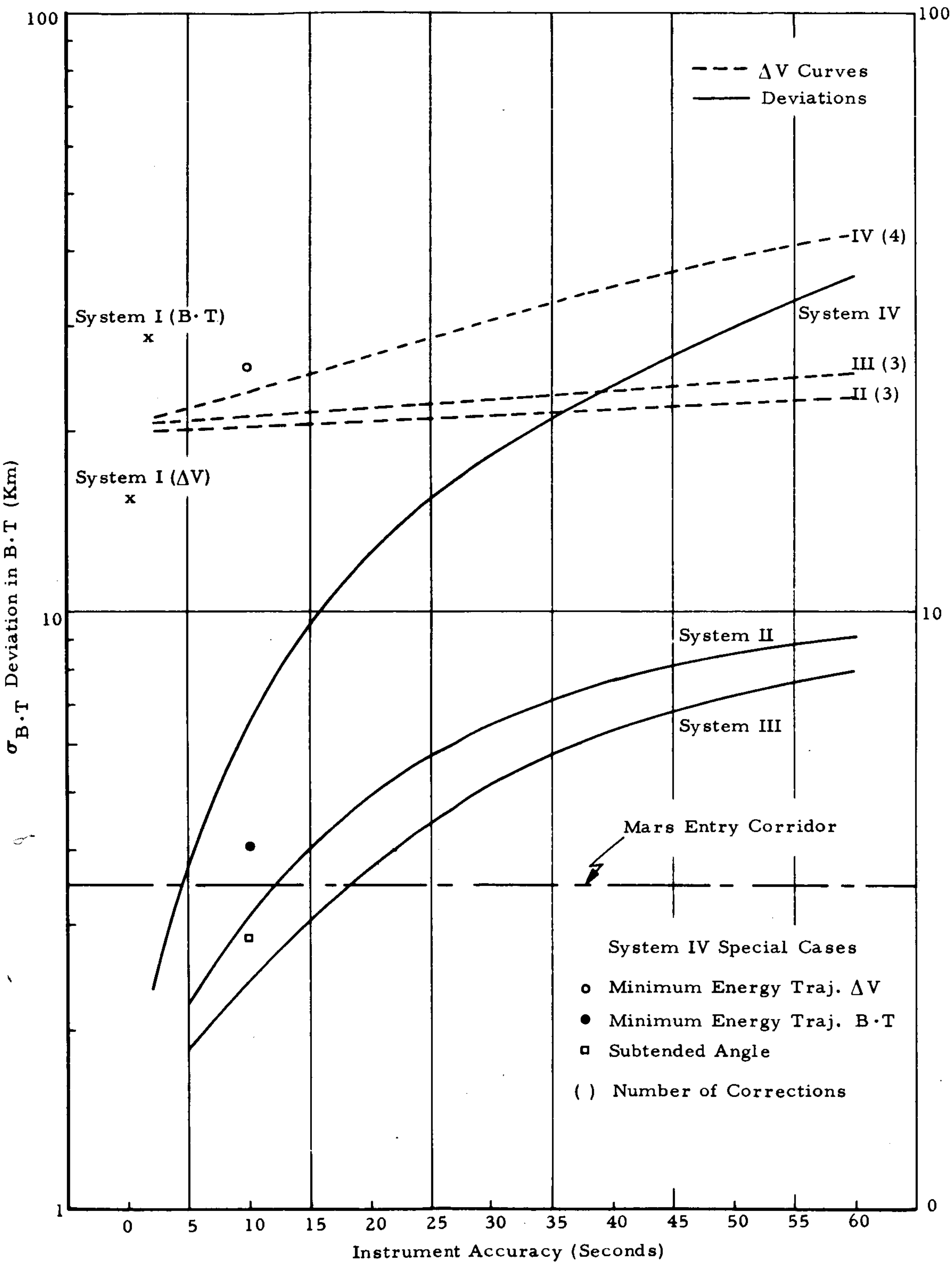

Figure 5-4A Summary of Systems Guidance Performance (B · T)

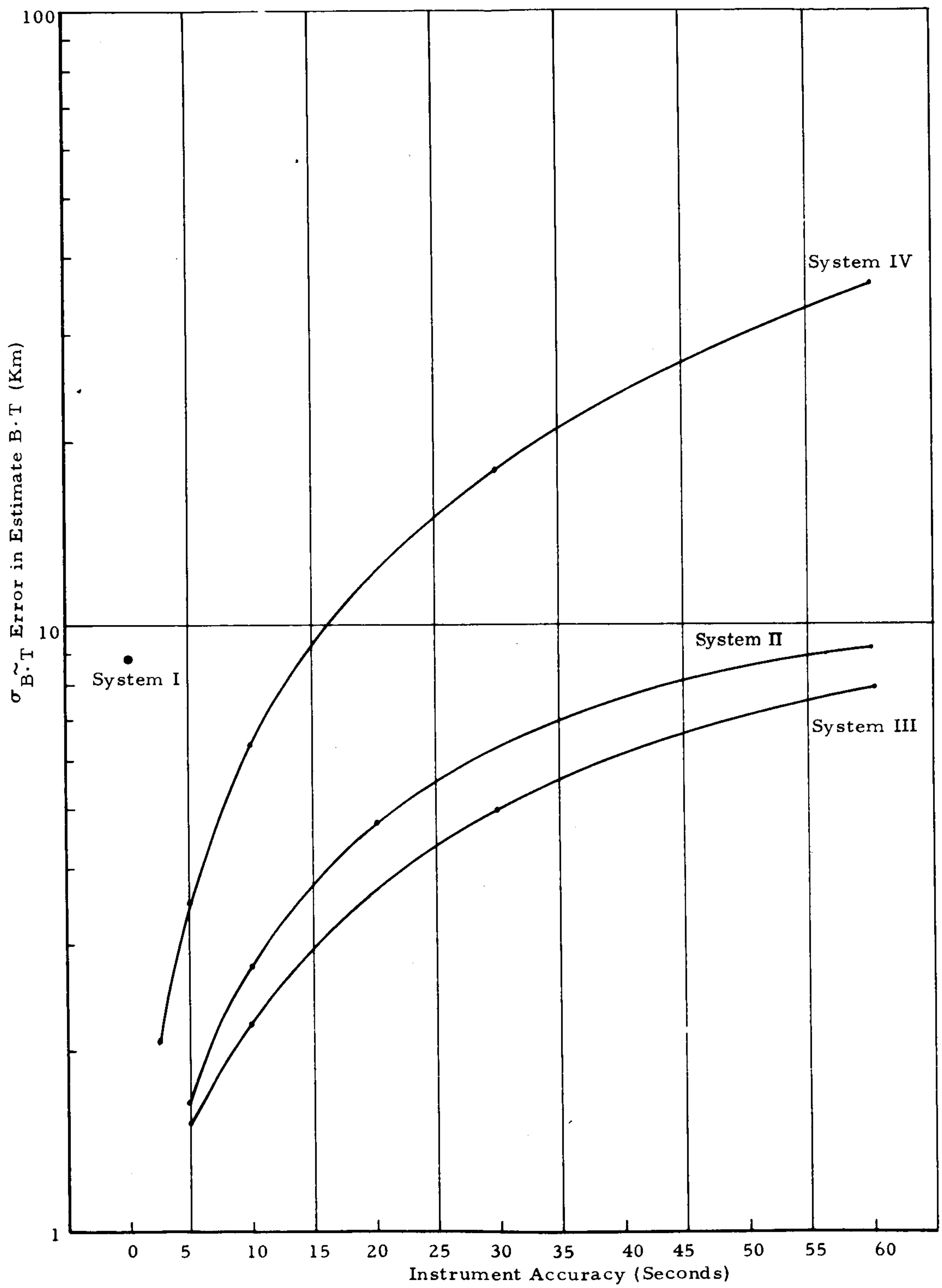

Figure 5-4B Summary of Navigation Performance, Time of Last Maneuver (B • T)

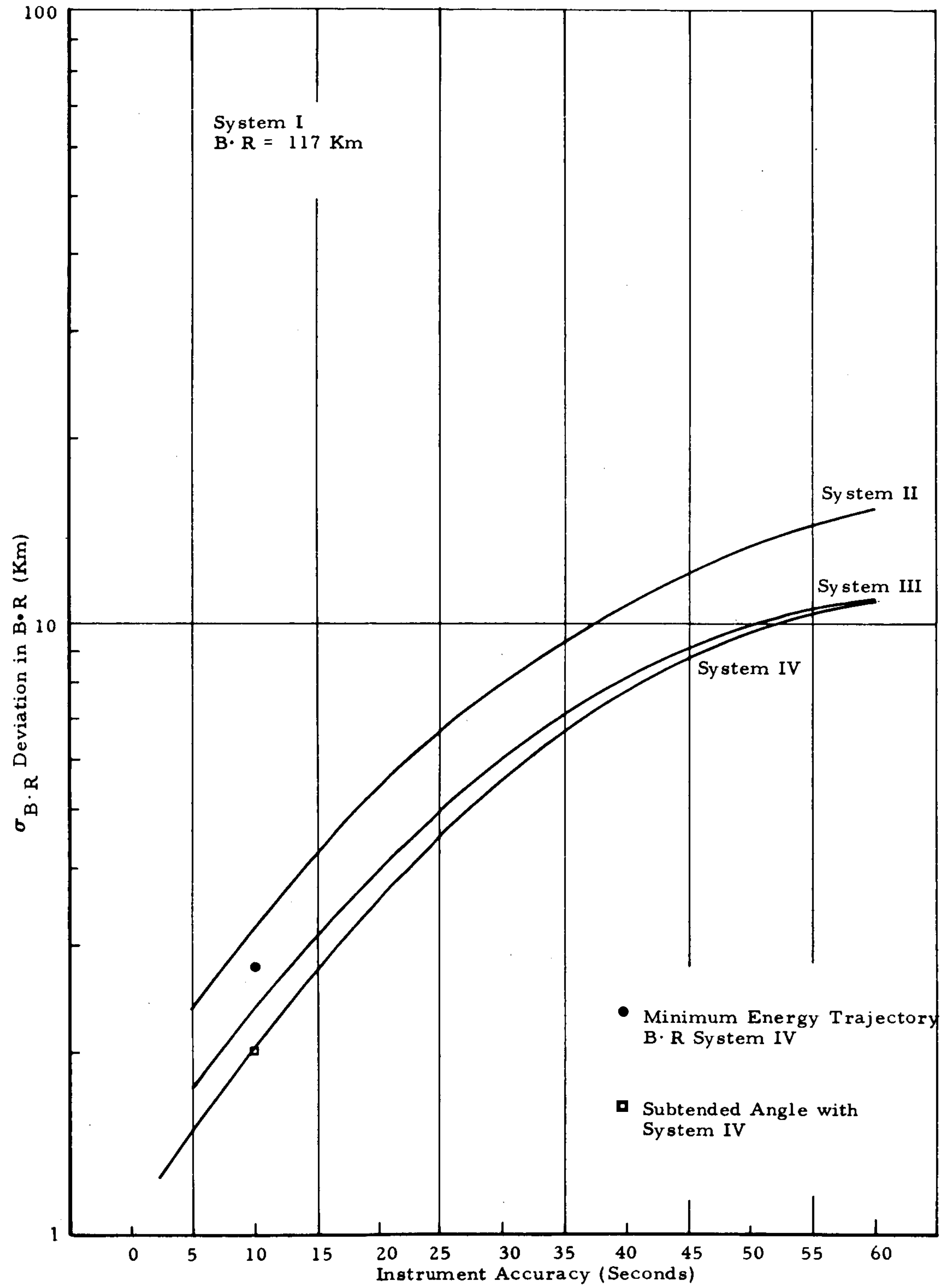

Figure 5-5A **Summary of Systems Guidance Performance (B · R)**

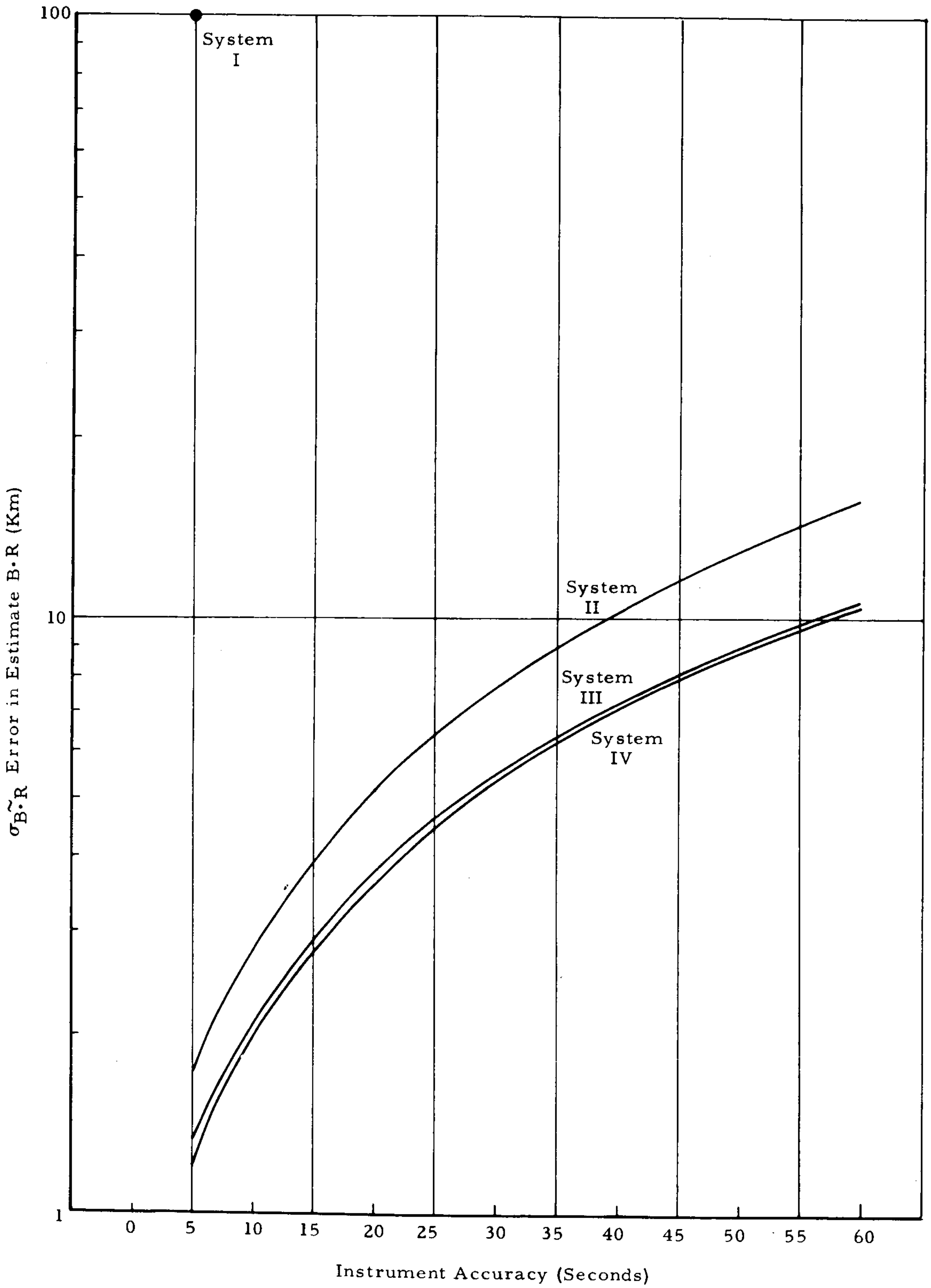

Figure 5-5B Summary of Navigation Performance, Time of Last Maneuver (B · R)

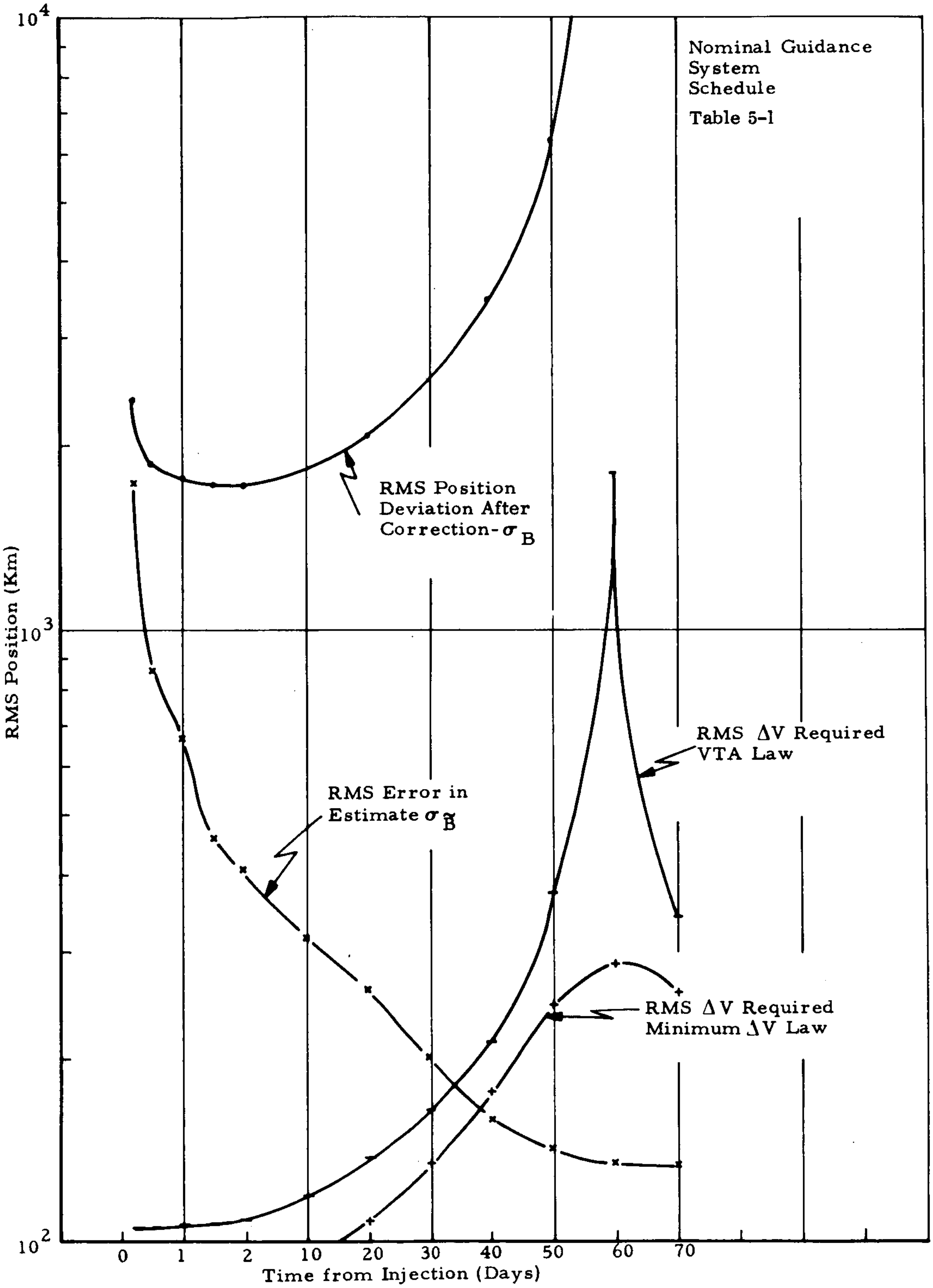

Figure 5-6 System I, First Correction Guidance Data

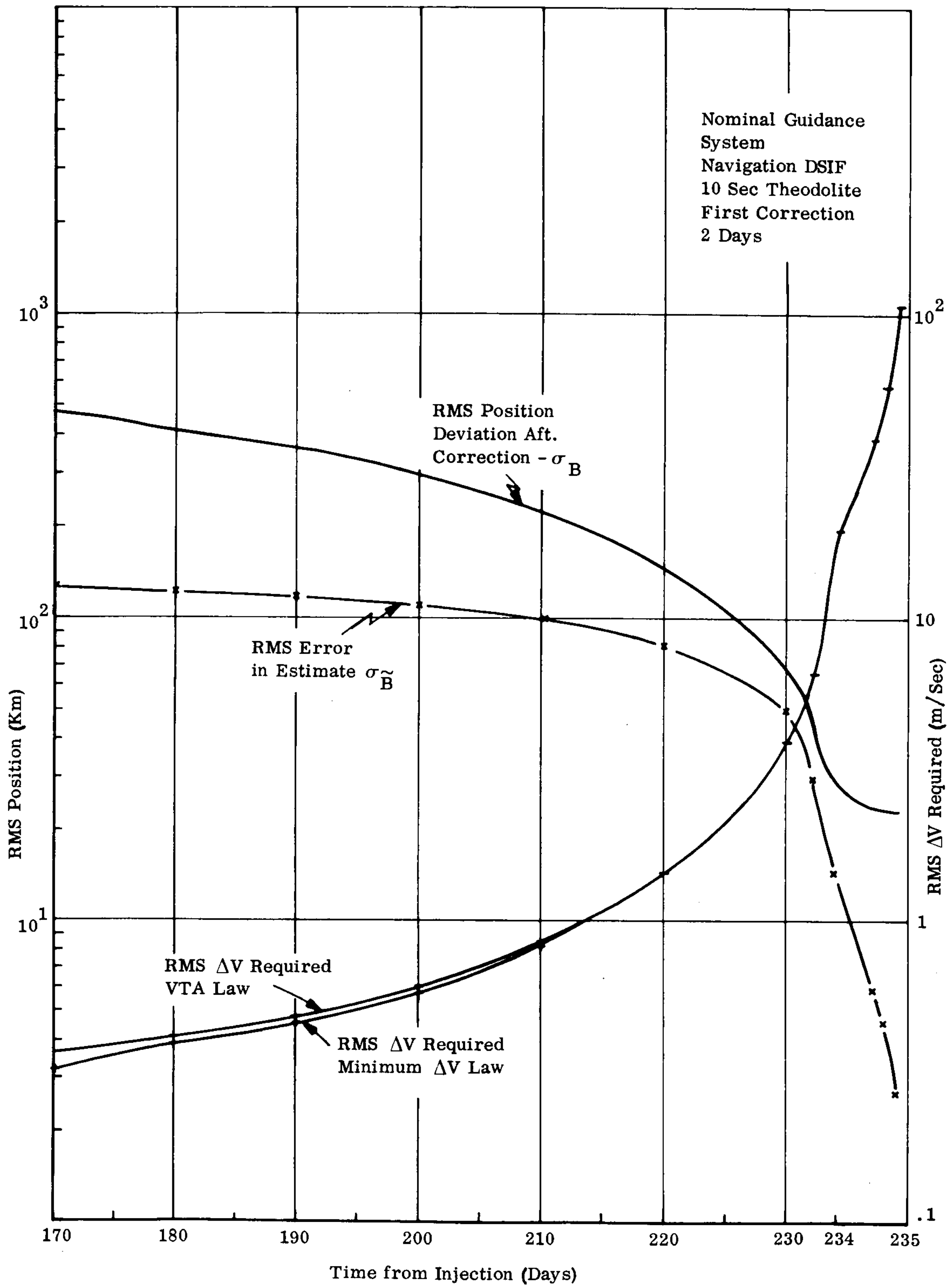

Figure 5-7A Systems II and III, Second Correction Guidance Data

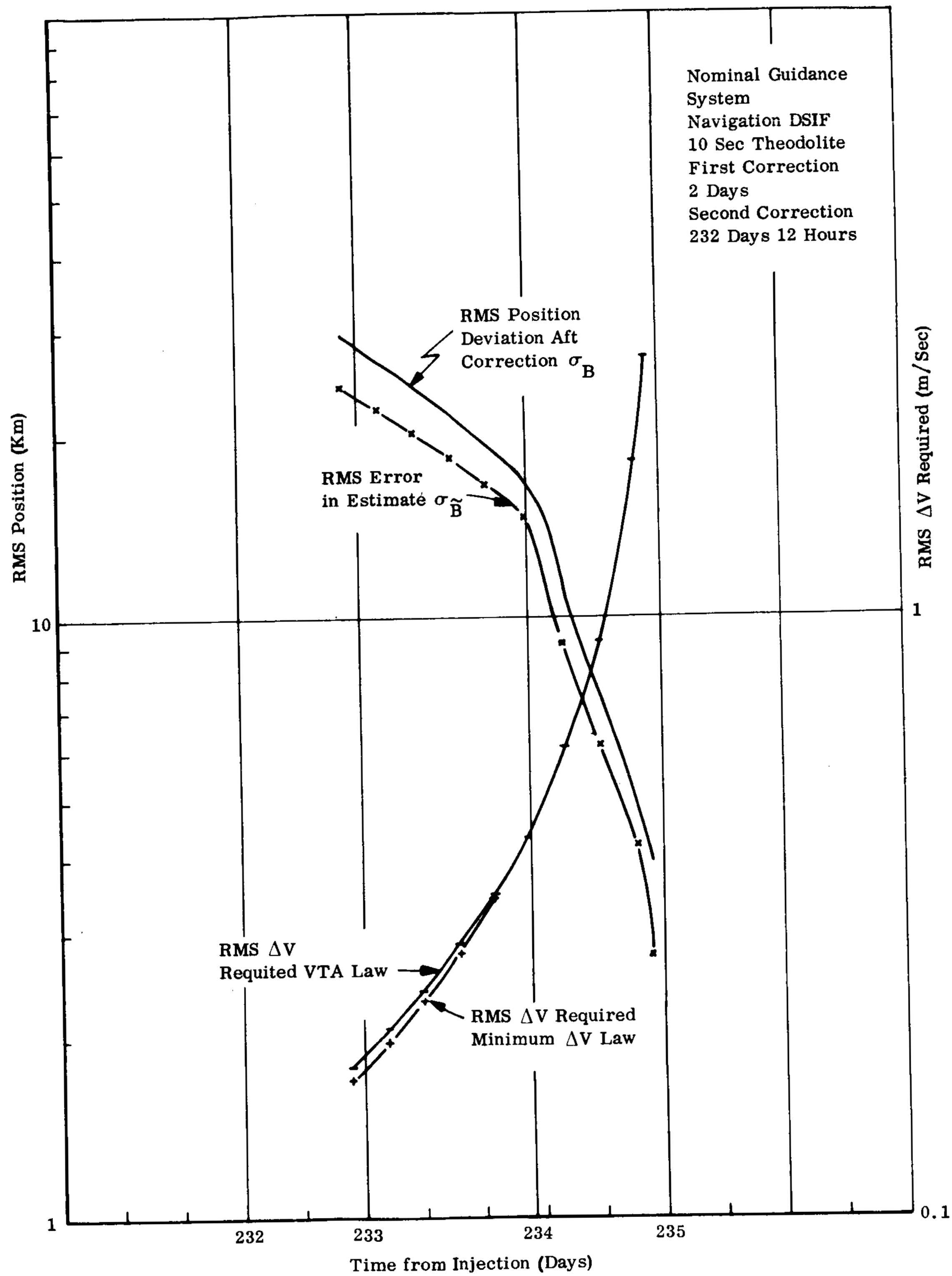

Figure 5-7B Systems II and III, Third Correction Guidance Data

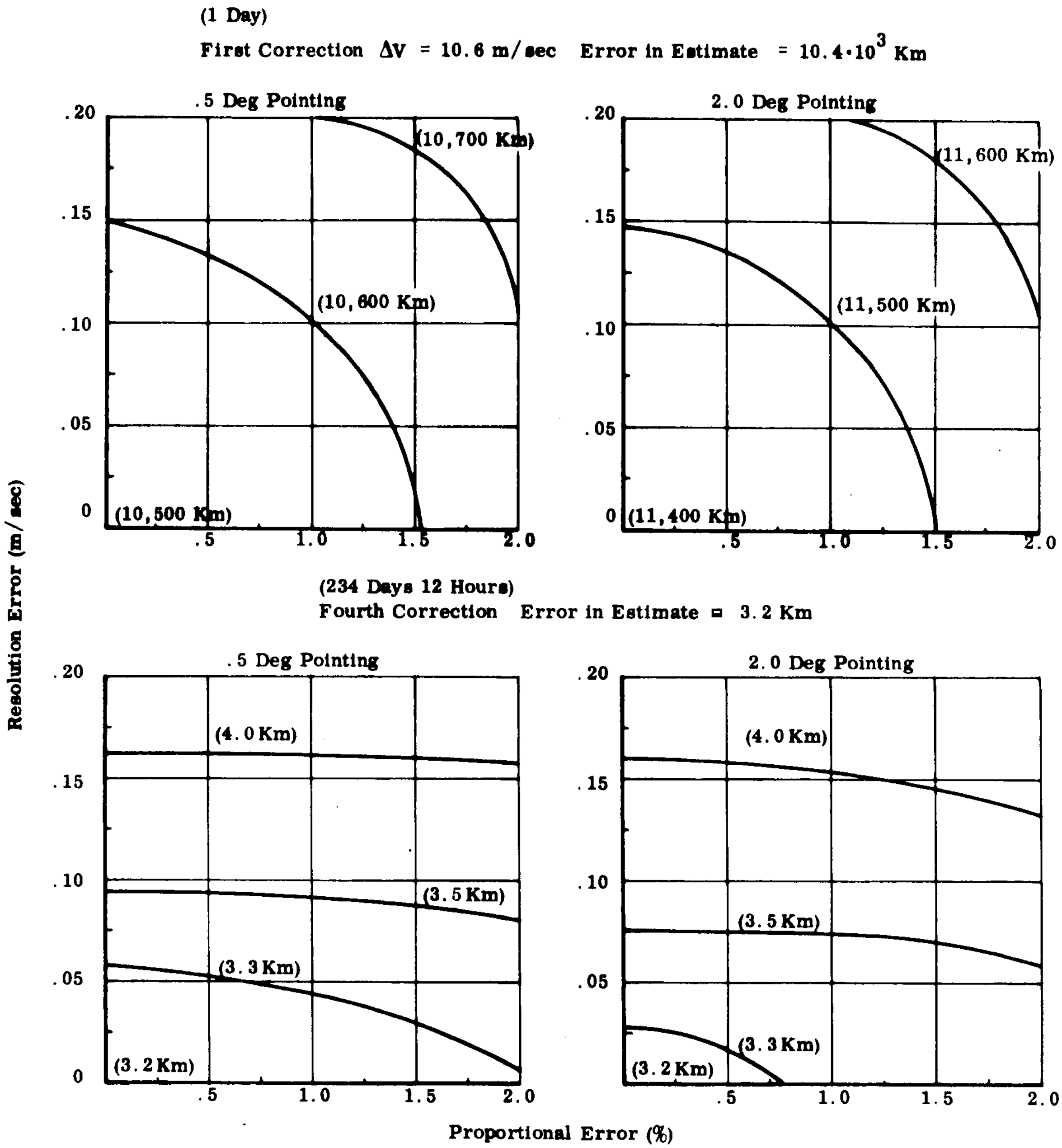

Figure 5-8 End-Point Deviations vs. Guidance System Errors - First and Fourth Corrections

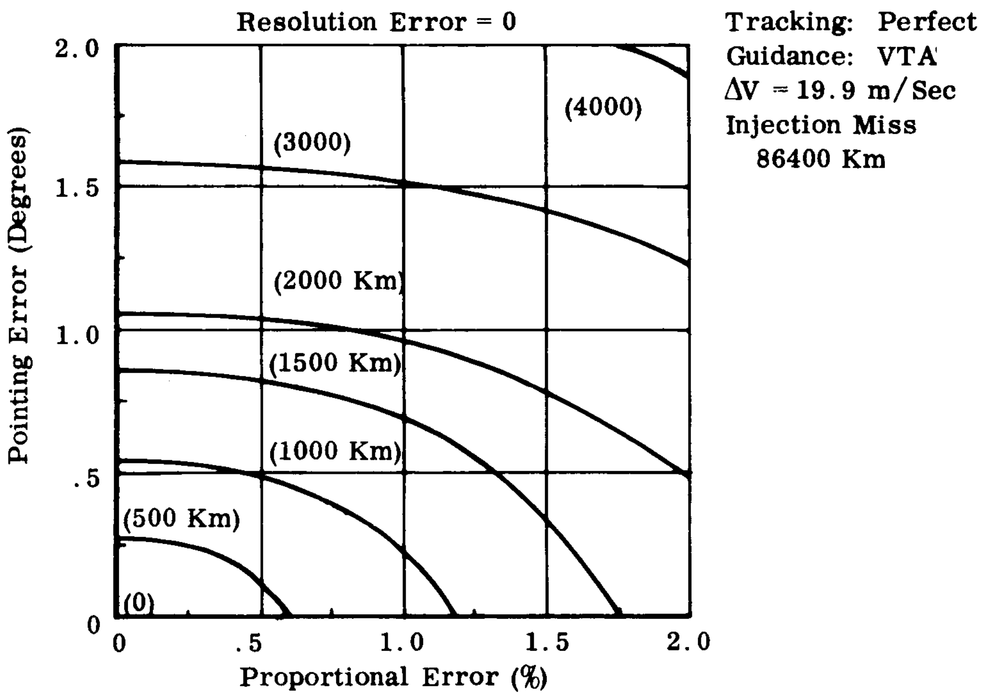

Figure 5-9A Single Correction Data - 180 Days

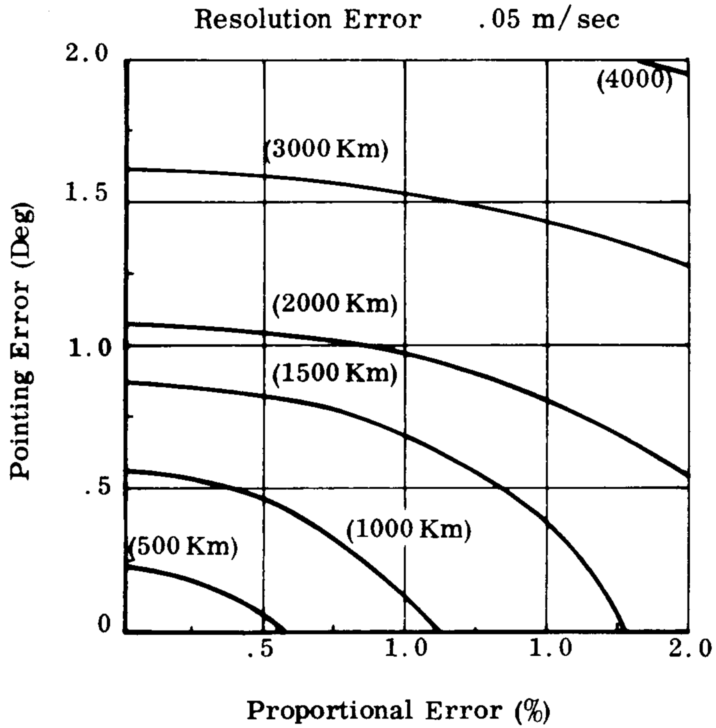

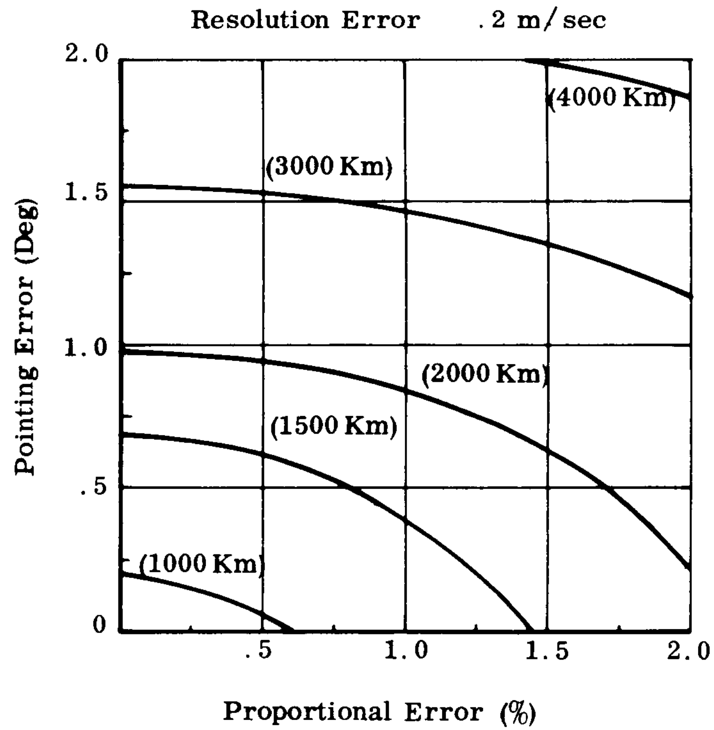

Figure 5-9B Single Correction Data - 180 Days Figure 5-9C

SECTION 6

MARS EARTH MIDCOURSE ANALYSIS

The results of the statistical error analyses of the navigation and guidance systems for the midcourse phase of the Mars-Earth return trajectory are described in this section. Since only Systems III and IV are reasonable choices for a manned Mars mission, it is these two systems that are discussed for the return phase. The results are obtained for an FTA guidance law with the perigee position constraints expressed in altitude, down range, and cross range coordinates. The covariance matrix of injection errors used on the return was a diagonal matrix with an RMS position deviation of 30 km and an RMS velocity deviation of 30 m/sec.

6.1 NAVIGATION SYSTEM

The navigation results for Systems III and IV are shown in Figure 6-1. System III utilized only the DSIF since the addition of onboard observations are of very small value on the return trajectory. System IV used a 10 arc-second theodolite. RMS error in estimate of the perigee position is primarily an error in the down range position. The perigee altitude estimate errors are 1.27 m/sec and 2.91 m/sec for System III and IV respectively. The guidance and navigation data for the two systems are summarized in Figure 6-2. These data have been obtained with the nominal guidance system and an FTA guidance law. System III is shown as a point on the graphs since the DSIF performance is good enough that onboard instruments are not needed for this system. The altitude deviation at perigee with System IV can be controlled to $\pm$ 3.5 km with a 4 arc-second insturment. This accuracy is adequate to hit an entry corridor at Earth.[5] For the special case that has assumed Moon observations with a 10 arc-second instrument, the data shows that these observations result in a significant reduction in both the estimation errors and the deviations at perigee. The system with a 10 arc-second instrument in this case is very nearly capable of hitting an entry corridor.

The use of a Venus swingby trajectory on the return leg showed the same guidance and navigation as the direct return trajectory. The velocity requirements increased from 110 meters/sec on the direct return to 250 meters/sec on the swingby return.

Table 6-1 presents the navigation and guidance system performance of System IV with a 10 arc-second insturment on two normal round trip Mars missions. The results are presented for the high energy round trips and the low energy with a Venus swingby return. These results indicate the system performance on the two trajectories is approximately the same. The only significant difference occurs in the velocity requirements on the swingby return trajectory.

6.2 GUIDANCE SYSTEM

The nominal guidance system on the return trajectory for an FTA guidance law controlled the end-constraints to within 10-20%.

The number of guidance corrections and their times are established with ΔV and deviation tradeoff data similar to that shown in Section 5.

The only significant guidance difference on the return trajectory is that the use of VTA and FTA guidance laws require approximately the same total ΔV. With FTA 100 meters/sec is required and 110 meters/sec with FTA. This is the result of a singularity (Figure 6-3) which occurs at 110 days when using a VTA guidance law. This causes the velocity requirements with a VTA guidance law to be significantly larger during the early part of the flight. The minimum ΔV curve shown in the figure indicates that in this case when V_∞ is not the third constraint, the singularity does not occur. However, at 170 days a second singularity occurs. This singularity is the result of the time anomaly to the target being 180 degrees at that time, and is seen to occur for both the VTA and minimum ΔV guidance laws.

The velocity requirements on the return leg are larger than the outbound primarily due to the different injection errors which have been used. The FTA velocity requirements on the outbound and return trajectories using the Earth injection errors for both are 56.89 m/sec and 56.85 m/sec respectively.

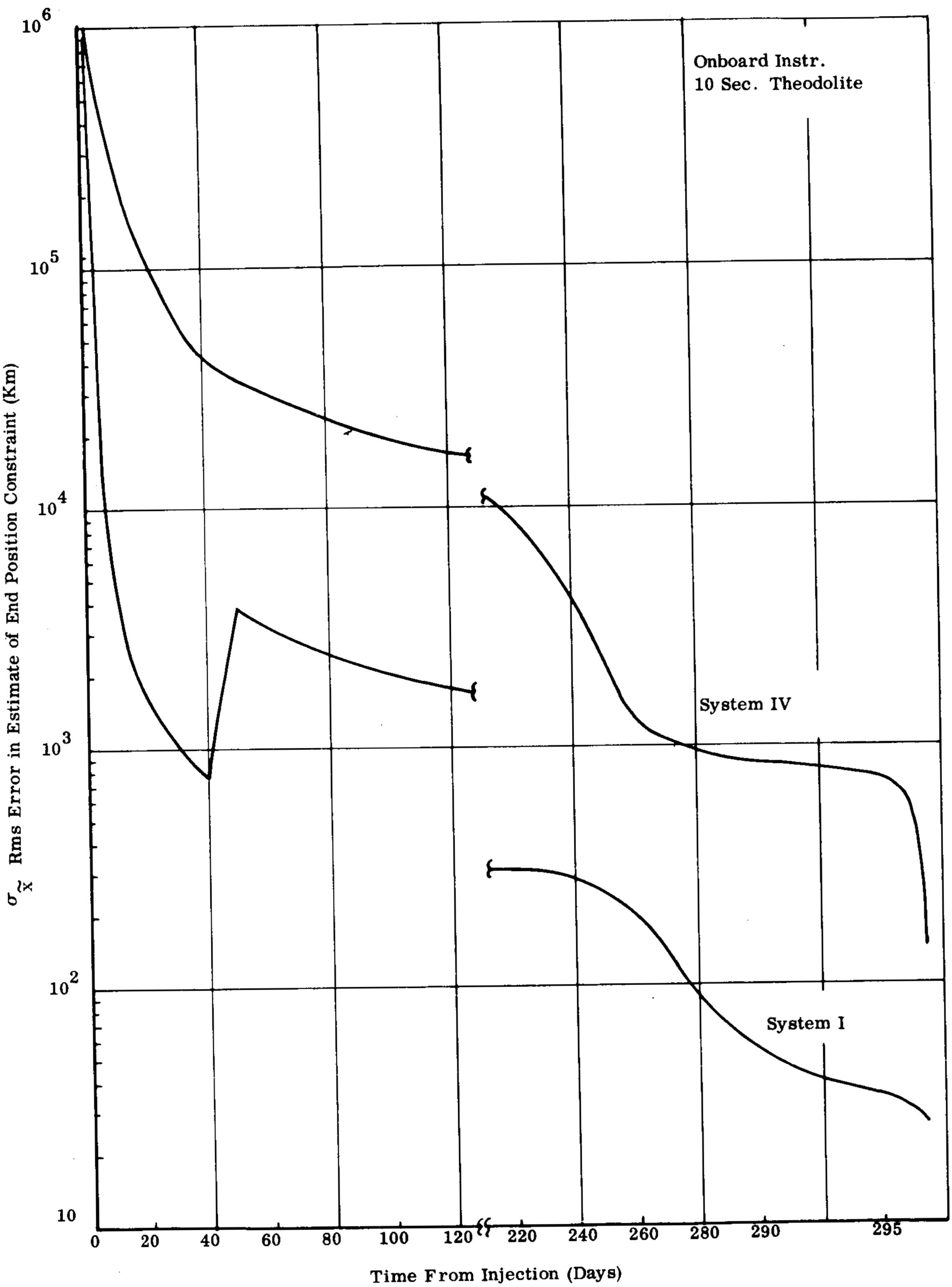

Figure 6-1 Navigation Data for Systems III and IV, Mars-Earth Trajectory

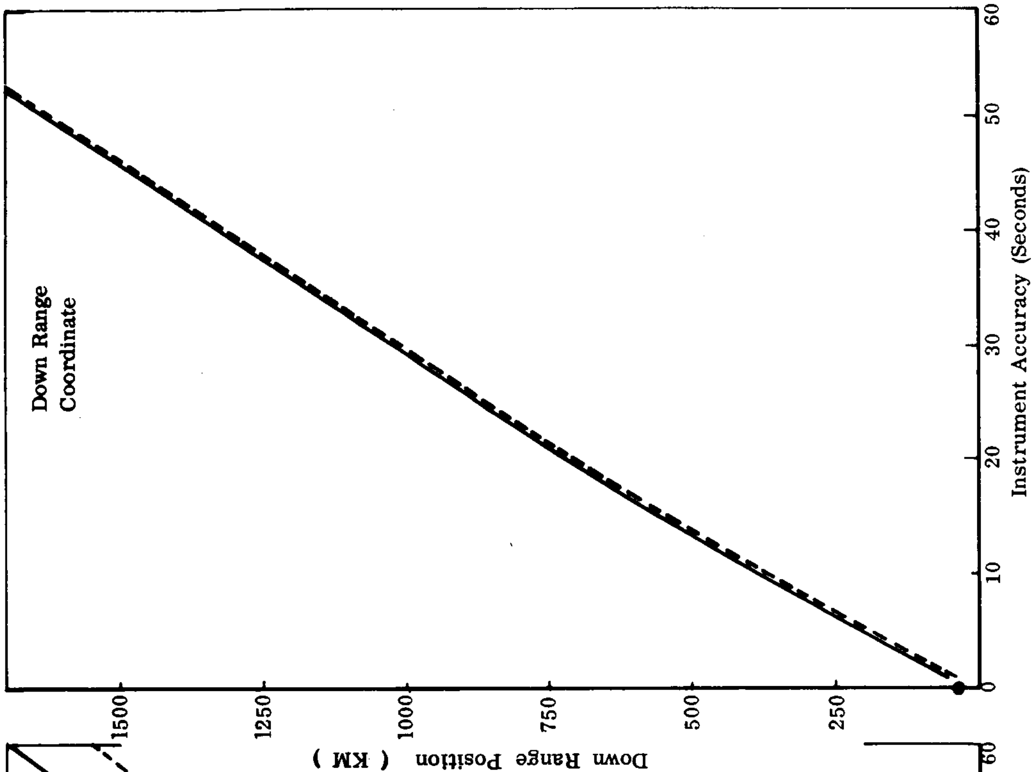

Figure 6-2B

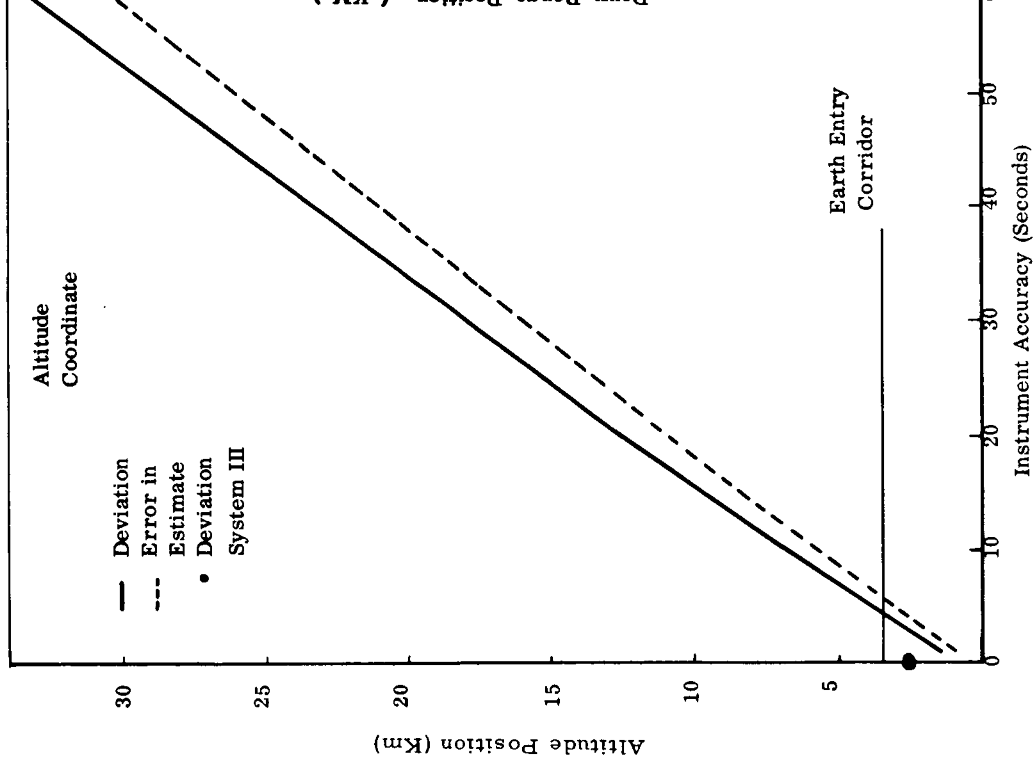

Figure 6-2A

Figure 6-2 System IV Guidance Performance

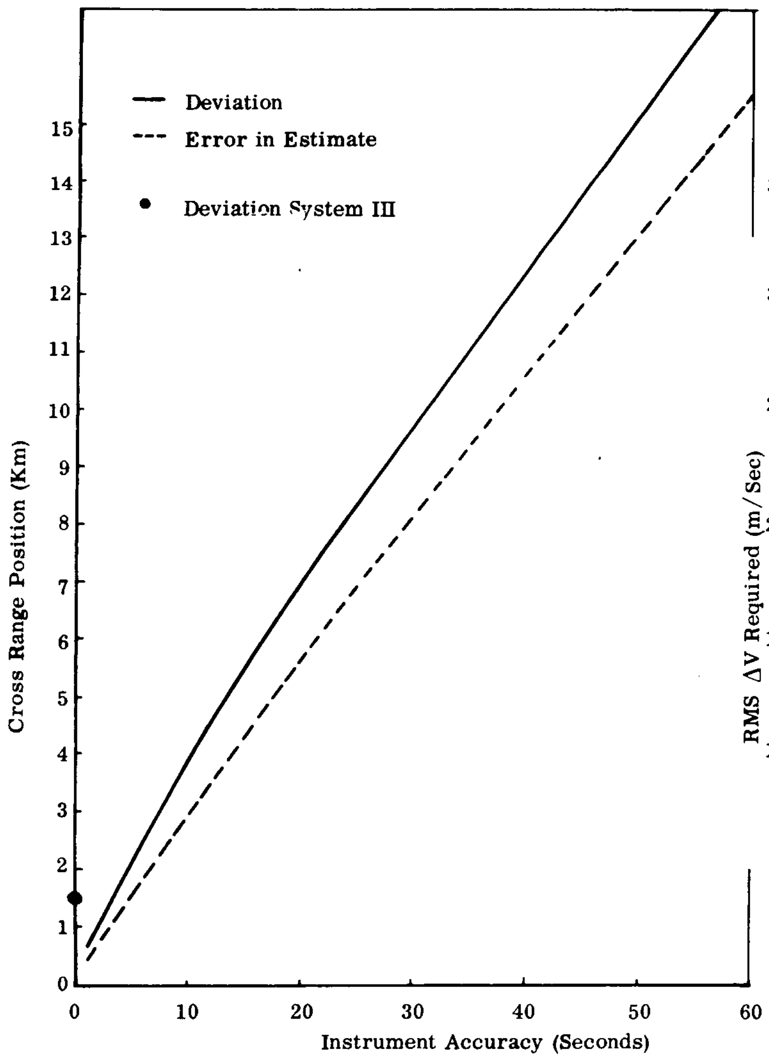

Figure 6-2C

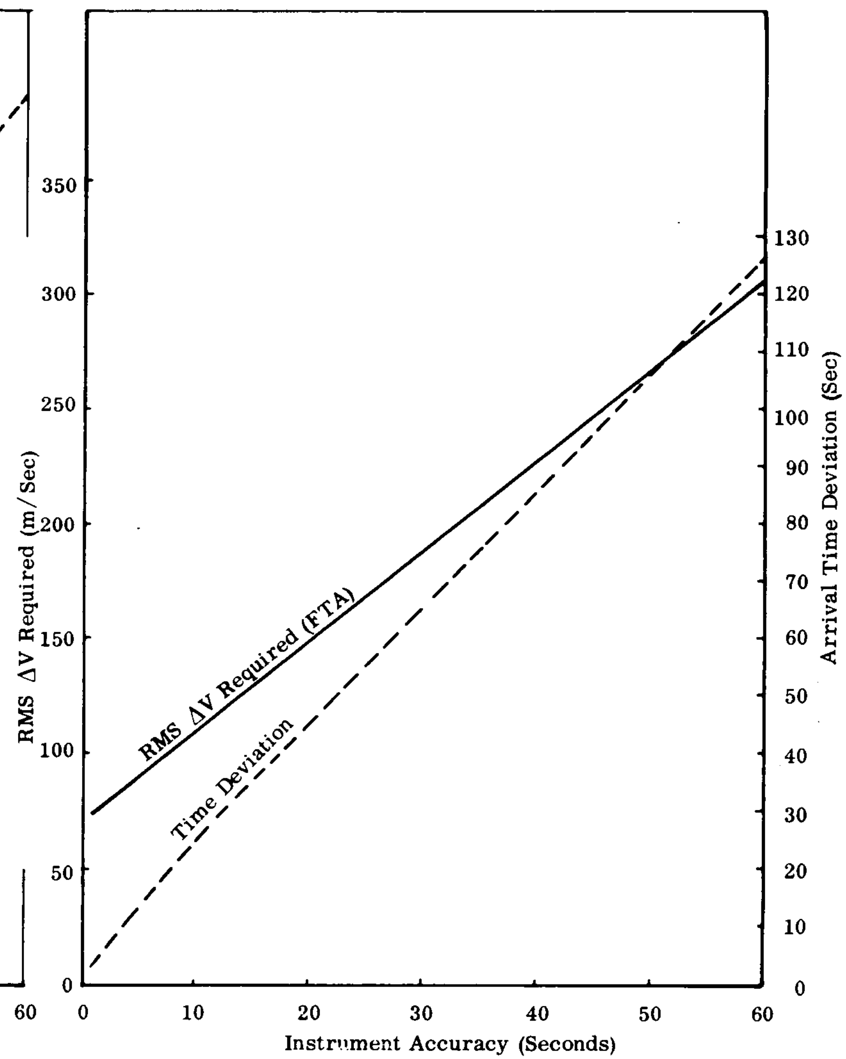

Figure 6-2D

Figure 6-2 System IV Guidance Performance (Cont'd)

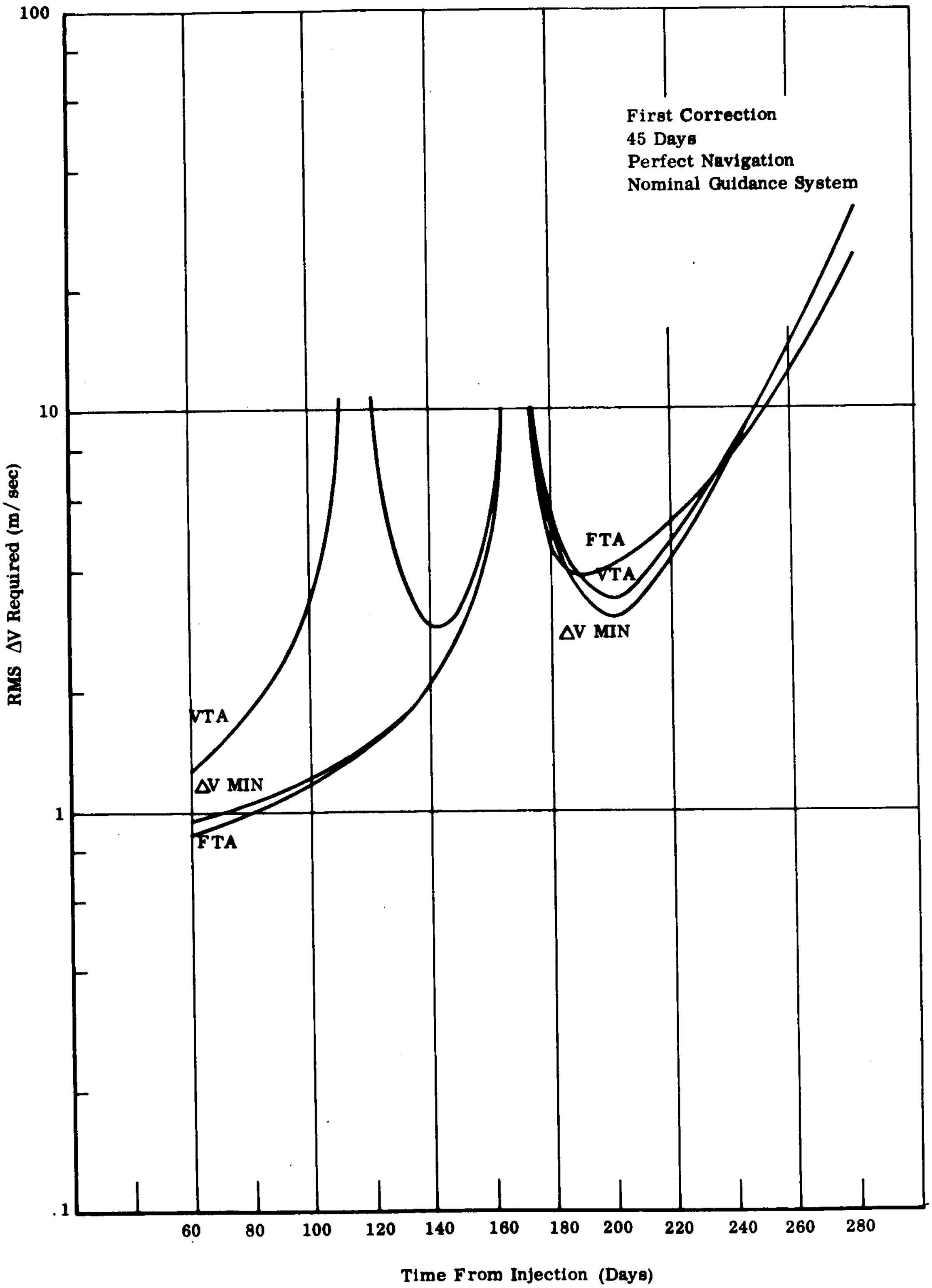

Figure 6-3 Second Correction Δv Requirements for Various Guidance Laws

TABLE 6-1A

TERMINAL CONDITIONS

HIGH ENERGY ROUND TRIP*

EARTH-MARS (VTA)		MARS-EARTH (FTA)	
Est B·T	6.38 Km	Est Alt	5.76 Km
Dev B·T	6.54 Km**	Dev Alt	6.80 Km**
Est B·R	1.99 Km	Est DR	383.00 Km
Dev B·R	2.01 Km	Dev DR	383.00 Km
Total ΔV	23.19 m/Sec	Est CR	2.91 Km
		Dev CR	3.86 Km
		Total ΔV	110.34 m/Sec

TABLE 6-1B

TERMINAL CONDITIONS

LOW ENERGY ROUND TRIP*

EARTH-MARS (VTA)		MARS-VENUS-EARTH (FTA)	
Est B·T	3.88 Km	Est Alt	5.17 Km
Dev B·T	4.07 Km**	Dev Alt	5.48 Km**
Est B·R	2.67 Km	Est DR	249.00 Km
Dev B·R	2.79 Km	Dev DR	250.00 Km
Total ΔV	25.86 m/Sec	Est CR	.88 Km
		Dev CR	1.18 Km
		Total ΔV	255.21 m/Sec

*10 Arc Second Theodolite
**Corridor Coordinate

SECTION 7

MARS ORBITAL ANALYSIS

The capability of the DSIF and onboard navigation systems to determine the Mars park orbit is discussed in this section. The orbital phase starts immediately after the retro maneuver and continues for 40 days. This phase of the mission has been studied independently of either of the mid-course phases. Initial uncertainties have been assumed that are larger than the values that would result from the outbound midcourse phase and the retro maneuver. No guidance corrections are considered and no specific mission requirements have been defined for this phase. The performance of the navigation systems is interpreted in terms of orbital elements, as well as the in-plane and out-of-plane components of position and velocity, for various orientations of the orbit.

The study of DSIF tracking shows that the RMS position and velocity uncertainties for the nominal park orbit after three days of tracking are 2 km and .025 km/sec respectively. The capability of the DSIF tracking, however, depends to a large extent on the inclination of the orbit plane with respect to the Earth-Mars line. Although azimuth, elevation, and range rate measurements have been assumed for this system, because of the large distance between Earth and Mars the only observation that provides accurate information is range-rate. This measurement provides information on the velocity components of the state that are along the LOS, and therefore the best results with DSIF tracking are obtained for large inclinations between the orbit plane and the tracker LOS. The smallest RMS uncertainties in position and velocity that have been obtained with DSIF tracking are shown in Figure 7-1 to be 400 km and .3 km/sec.* These values resulted from an orbit that was inclined 90^{o} to the Earth-Mars line. The effect of the vehicle occultation by Mars has also been determined. For the orbit that results in the longest occultation time, the increase in position and velocity uncertainties over the case where no occulation occurs is 30 percent and 25 percent, respectively.

*These values are obtained on the 4th orbit.

A summary of the results of evaluating seven different navigation systems for the nominal park orbit is shown in Table 7-1. These systems include DSIF,DSIF-sextant, DSIF-onboard radar, sextant, onboard radar, subtended angle, and sextant-subtended angle measurements. As shown in the table, the most accurate orbit determination is obtained with the DSIF-sextant system. The RMS uncertainties in position and velocity with these observations are .2 km and .17 m/sec respectively. The performance of a system with either sextant or sextant and subtended angle measurements is also quite accurate and results in RMS uncertainties of .75 km and .6 m/sec. The performance of systems that make use of sextant observations is in general good because these measurements are capable of determining both the in-plane and out-of-plane components of the position and velocity uncertainties. The results of DSIF-onboard radar, onboard radar, and subtended angle measurements, also shown in Table 7-1, are considerably poorer than the sextant measurements.

A composite summary of the navigation capabilities of the seven systems for determining the six orbital elements, is given in Table 7-2. These data also show that the best performance is obtained with DSIF-sextant observations.

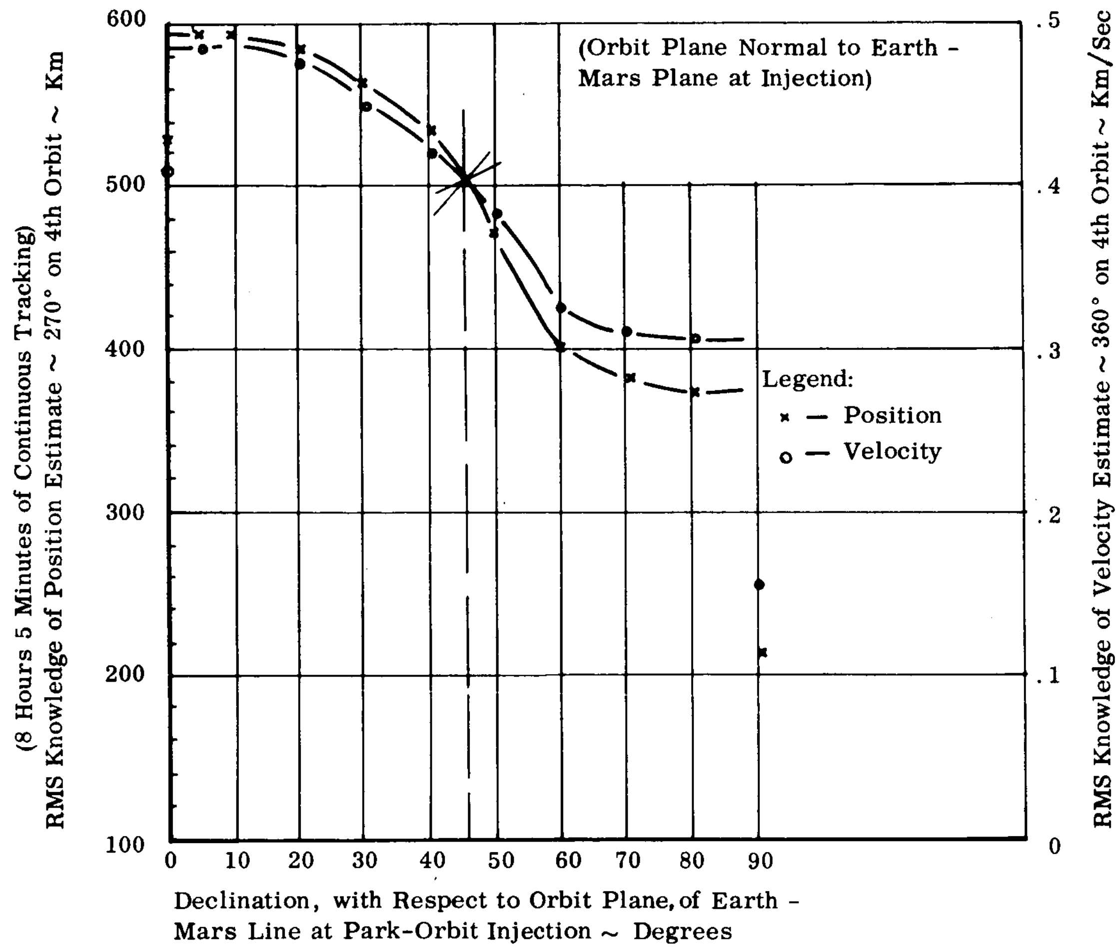

Figure 7-1 RMS Position and Velocity Estimate Knowledge at 270 Degrees True Anomaly on the Fourth Orbit vs. Earth-Mars Declination Angle

TABLE 7-1

FTAV RESULTS*

Conditions at 3 days	DSIF	Sextant	Radar	Subtense	DSIF-Radar	Sextant-Subtense	DSIF-Sextant	Initial Conditions
Secular Term RMS	1×10^{1}	7.5×10^{-1}	1.375×10^{3}	1.375×10^{3}	1×10^{1}	7.5×10^{-1}	2×10^{-1}	1.732×10^{3} Km
Position Actual (72 hours)	1.81×10^{1}	7.7×10^{-1}	1.431×10^{3}	1.433×10^{3}	2.17×10^{1}	7.58×10^{-1}	3.54×10^{-1}	
Secular Term RMS	7.5×10^{-3}	6×10^{-4}	1.09×10^{0}	1.09×10^{0}	7.5×10^{-3}	6.0×10^{-4}	1.7×10^{-4}	1.732×10^{0} KM/Sec.
Velocity Actual (72 hours)	1.91×10^{-3}	5.67×10^{-4}	1.05×10^{0}	1.04×10^{0}	2.28×10^{-3}	5.68×10^{-4}	6.44×10^{-6}	
RMS Position Components Actual (72 hours) N	4.19×10^{-2}	1.77×10^{-1}	1.46×10^{1}	1.48×10^{1}	5.08×10^{-2}	1.56×10^{-1}	6.51×10^{-3}	1×10^{3} KM
V	1.93×10	6.59×10^{-1}	7.85×10^{2}	7.89×10^{2}	2.32×10^{0}	6.50×10^{-1}	4.70×10^{-2}	1×10^{3} KM
W	1.8×10^{1}	3.57×10^{-1}	$1.000\ 10^{3}$	$1.000\ 10^{3}$	2.15×10^{1}	3.57×10^{-1}	3.51×10^{-1}	1×10^{3} KM
RMS Velocity Components Actual (72 hours) N	1.55×10^{-3}	4.69×10^{-1}	6.27×10^{-1}	6.30×10^{-1}	1.85×10^{-3}	4.75×10^{-1}	3.63×10^{-5}	1×10^{0} KM/Sec.
V	1.94×10^{-5}	1.42×10^{-1}	3.51×10^{-4}	1.33×10^{-3}	2.21×10^{-5}	1.25×10^{-1}	5.10×10^{-6}	1×10^{0} KM/Sec.
W	1.12×10^{-3}	2.84×10^{-1}	8.4×10^{-1}	8.4×10^{-1}	1.32×10^{-3}	2.84×10^{-1}	5.29×10^{-5}	1×10^{0} KM/Sec.

*Nominal Trajectory

TABLE 7-2

SYSTEM COMPARISON - ALL SYSTEMS AND SPECIAL DSIF CASES

	SPECIAL TRAJECTORY			NOMINAL TRAJECTORY						
	DSIF (R.W)=0	DSIF (R.W)=1	(RR)ONLY DSIF (R.W.)=1	DSIF	SEXTANT	RADAR	SUBTENSE	DSIF-RADAR	SEXTANT SUBTENSE	DSIF-SEXTANT
e	10^{-4} $3x10^{1}$ 1	$2x10^{-4}$ $5x10^{1}$ 2	$2.5x10^{-4}$ $6x10^{1}$ 2	$1.25x10^{-5}$ $3x10^{0}$ 0	10^{-4} $3x10^{1}$ 1	$2.5x10^{-4}$ $6x10^{1}$ 2	$3x10^{-4}$ $8x10^{1}$ 2	$2x10^{-5}$ $5x10^{0}$ 1	10^{-4} $3x10^{1}$ 1	$4x10^{-6}$
q	$4x10^{-1}$ KM $2x10^{1}$ 1	1 $6x10^{1}$ 2	1 $6x10^{1}$ 2	$5x10^{-2}$ $3x10^{0}$ 0	$4x10^{-1}$ $2x10^{1}$ 1	$7x10^{1}$ $4x10^{1}$ 1	1 $6x10^{1}$ 2	$7x10^{-2}$ $4x10^{0}$ 0	$3.5x10^{-1}$ $2x10^{1}$ 1	$1.75x10^{-2}$
a	$2x10^{-1}$ KM $1x10^{2}$ 2	$1x10^{-1}$ $7x10^{1}$ 2	$5.5x10^{-2}$ $4x10^{1}$ 1	$1.75x10^{-2}$ $1x10^{1}$ 1	$1.5x10^{-2}$ $1x10^{1}$ 1	$9x10^{-1}$ $6x10^{2}$ 3	$3x10^{-1}$ $2x10^{2}$ 2	$2.5x10^{-2}$ $2x10^{1}$ 1	$1.75x10^{-2}$ $1x10^{0}$ 0	$1.5x10^{-3}$
Ω	$9.5x10^{0}$ RAD $1x10^{3}$ 3	$4x10^{-4}$ $4x10^{-2}$ -2	$1.75x10^{-4}$ $2x10^{-2}$ -2	$5.25x10^{-1}$ $6x10^{1}$ 2	10^{-2} $1x10^{0}$ 0	3.25 $3x10^{2}$ 2	$1.75x10^{0}$ $2x10^{2}$ 2	$6x10^{-1}$ $6x10^{1}$ 2	10^{-2} $1x10^{0}$ 0	$9.5x10^{-3}$
i	2.5 RAD $2x10^{3}$ 3	$2.75x10^{-3}$ $2x10^{0}$ 0	10^{-3} $7x10^{-1}$ 0	$7.25x10^{-2}$ $5x10^{1}$ 2	$5x10^{-3}$ $3x10^{0}$ 0	1.5 $1x10^{3}$ 3	$5x10^{-1}$ $3x10^{2}$ 2	$8x10^{-2}$ $5x10^{1}$ 2	$5x10^{-3}$ $3x10^{0}$ 0	$1.5x10^{-3}$
ω	$3.5x10^{3}$ RAD $1x10^{3}$ 3	$5.5x10^{-1}$ $2x10^{0}$ 0	$4.5x10^{-1}$ $2x10^{0}$ 0	$1x10^{1}$ $4x10^{1}$ 1	$5x10^{-1}$ $2x10^{0}$ 0	10^{3} $4x10^{3}$ 3	2 $8x10^{0}$ 1	$1.5x10^{1}$ $6x10^{1}$ 2	$5x10^{-1}$ $2x10^{0}$ 0	$2.5x10^{-1}$

NOMENCLATURE: Standard Deviation
Ratio (i.e. System/DSIF-SEX)
Order of Magnitude By Which
DSIF-Sextant is Superior

SECTION 8

RECOMMENDATIONS

Additional study areas which would extend the scope of the present study, and which are considered to be important for defining the navigation and guidance requirements of an interplanetary mission, are the following:

a. Precision Trajectory. The results which are obtained in this study with a patched conic trajectory should be verified with the use of a precision trajectory.

b. Bias Errors. The influence of bias error sources which are neglected in this study should be evaluated. These errors include uncertainties in the physical constants (mass of the Sun, oblateness of Mars, mass of Mars, etc.), measurement instrument biases, on board clock bias, and tracker station location errors.

c. Filtering Technique. The study has assumed the use of a Kalman filter in the data processing. The various other filtering techniques should be evaluated and, in particular, consideration should be given to their onboard implementation.

d. Beacons. The importance of having beacons on Mars should be evaluated for the approach phase of the mission, terminal maneuvering phase and the orbital phase.

e. Terminal Maneuvers. The requirements for inertial equipment in the guidance system should be determined for the retro maneuver (powered and/or atmospheric) and the powered flight out of the Mars orbit. A retro analysis is also required at perigee on the return.

f. Onboard Computer. The design of the onboard computer should be studied to determine means of trading off speed for reliability (500 to

600-day missions). Also, techniques for simplifying calculations for estimating and predicting the state should be investigated. This investigation should include the effects of truncation errors in the computer.

g. Mars Orbit. The navigation requirements in orbit should be determined in terms of specific mission objectives. The influence of the oblateness of Mars on these requirements should be evaluated. The errors resulting from park orbit navigation and the burning maneuver out of orbit should be evaluated in terms of their effect on the return trajectory computations and performance.

h. Venus Swingby. The Venus swingby mission should be studied in detail because of its apparent importance in a round-trip Mars mission.

REFERENCES

1. Interplanetary Navigation and Guidance Study, WDL-TR2629, Vol. II, Philco WDL, Palo Alto, California, 30 October 1965.

2. Kizner, W., A Method of Describing Miss Distance for Lunar Interplanetary Trajectories, JPL Publication No. 674, 1 August 1959.

3. Battin, R. N., Astronautical Guidance, McGraw-Hill Book Co., 1964.

4. Rohde, P. J., The Scheduling of Measurements for Analysis of an Onboard Navigation System, WDL-TR2600, October 1965 (to be published as NASA contractor report).

5. Manned Mars Mission Study, Report for NASA, Ames, Contract No. NAS 2-1409, By TRW, STL, Redondo Beach, Calif., 28 March 1964.

6. "Results on Physical Constants and Related Data from the Radio Tracking of Mariner (Venus) and Ranger III - VII Missions", W. L. Spogren and D. W. Trask, Journal of Spacecraft and Rockets, Volume 2, Number 5, September - October 1965.

7. Stern, R. G., "Interplanetary Midcourse Guidance Analysis", MIT Experimental Astronomy Laboratory TE-5, Appendix 0, May 1963.